Normal, ICAR and photomediated butadiene-ATRP with iron complexes

Vignesh Vasu, [ID] Joon-Sung Kim, Hyun-Seok Yu, William I. Bannerman, Mark E. Johnson and Alexandru D. Asandei [ID] *

The ligand (L) and halide effects of a series of iron complexes (FeX$_2$ or FeX$_3$, X = Cl, Br)/L supported by carbon (Cp$_2$Fe$_2$(I)(CO)$_4$ > Cp$_2$Fe > Fe(CO)$_5$ > (Ph$_2$PCp)$_2$Fe), nitrogen (phthalocyanine ≫ bpy ≥ MeO-bpy ≫ PMDETA > phen), halide (FeX$_m$Y$_{4-m}$/Bu$_4$N, X, Y = Cl ≫ Br > I), oxygen (12-crown-4 ≫ 15-crown-5 ≥ dibenzo-18-crown-6) and phosphorous (P[Ph(2,4,6-OMe)$_3$]$_3$ > P(t-Bu)$_3$ ≫ P(n-Bu)$_3$, PPh$_3$, P[Ph(4-CF$_3$)]$_3$, P(C$_6$F$_5$)$_3$) ligands, as well as ligand-free FeX$_3$, were evaluated in the normal, ICAR, and photo-ATRP of butadiene (BD) initiated from bromoesters, α,α-dichloro-p-xylene, or FeX$_3$ in toluene at 110 °C. Good polymerization control was observed in many cases, and two clear trends *i.e.* P[Ph(OMe)$_3$]$_3$ ≫ Bu$_4$NX > crown ethers > amines > C-ligands and FeCl$_2$, FeCl$_3$ ≫ FeBr$_2$, FeBr$_3$ occur consistently across all polymerizations. These effects correlate with the higher stability of the allyl PBD-Cl *vs.* PBD-Br chain ends and with FeCl$_3$ likely being a better deactivator than FeBr$_3$. Conversely, while basic enough to reduce FeX$_3$, P[Ph(2,4,6-OMe)$_3$]$_3$ is not nucleophilic enough to quaternize PBD-X in the apolar toluene and successfully enables a faster activation/deactivation equilibrium than all other ligands. As such, *e.g.* N-ATRP with [BD]/[R−Br]/[FeCl$_3$]/P[Ph(2,4,6-OMe)$_3$]$_3$ = 100/1/2/3 affords a linear M_n *vs.* conversion profile with PDI as low as 1.15–1.2 and a halide chain end functionality (CEF) = 0.65 at up to 50% conversion. While controlled polymerizations occur in photo-ATRP even without ligand and initiator, photoirradiation of catalytic N-ATRP with BD/R−Br/FeCl$_3$/P[Ph(2,4,6-OMe)$_3$]$_3$ = 100/1/0.05/0.15 significantly improves the rate (×10 *vs.* dark), conversion (up to 70%) and X-CEF (0.9) *via* the additional initiation afforded by FeX$_3$ photolysis, albeit with a slight PDI increase to ~1.4. Thus, Fe-mediated BD-ATRP is achievable, and the rational selection of the polymerization variables enables minimization of side reactions and the successful synthesis of well-defined PBD with a wide range of molecular weights, narrow PDI and reasonably high X-CEF, suitable for the preparation of *e.g.* block copolymers.

Introduction

The scale of the industrial synthesis of homo, random and block copolymers containing conjugated 1,3-dienes (butadiene, (BD), isoprene (ISO), dimethylbutadiene, (DMBD), and chloroprene (ClP)) reaches up to billions of pounds per year, which testifies to their importance.[1,2] However, while radical emulsion polymerization can be used for the preparation of rubbers, coatings, adhesives, and high impact materials based on random copolymers of dienes with acrylonitrile (AN) or styrene (St),[1] the corresponding thermoplastic elastomer blocks are prepared by expensive, air and water sensitive anionic or coordination[3] polymerizations that require strict

reaction conditions, and offer only a limited selection of initiator and chain end functionalities.[1]

As such, water tolerant, inexpensive controlled radical polymerizations (CRPs, which proceed with a linear dependence of M_n on conversion, narrow polydispersity (PDI) and high chain end functionality (CEF)),[4–7] would be desirable. Conversely, diene radical polymerizations include a series of drawbacks such low monomer boiling points (b_p^{BD} = 4.4 °C, b_p^{ISO} = 34 °C), Diels–Alder (DA) cycloadditions[8] (BD to 4-vinyl cyclohexene[8,10,14] and ISO to limonene) as well as chain transfer to the weak allylic Hs which leads to branching/crosslinking at high conversion. Moreover, the characteristic diene radical propagation mode, entailing the equilibrium of the prevailing primary 1,4-radical with other allylic delocalized resonance isomers,[9] leads to mixtures of constitutionally isomeric 1,2-, 3,4- or 1,4-*cis/trans* main chain connectivities,[1] and to the lowest radical propagation rate constants (k_p) of typical radical monomers,[1,4,9] ($k_p^{acrylates}$ > 10^4 > $k_{p,5C}^{Sty}$ ~ 180 > $k_{p,5C}^{BD}$ ~ 150 >

Institute of Materials Science and Department of Chemistry,
University of Connecticut, 97 North Eagleville Rd, Storrs, CT, 06269-3139, USA.
E-mail: alexandru.asandei@uconn.edu; Tel: +860-486-9062

$k_{p,5C}^{ISO} \sim 125$ M^{-1} s^{-1}).[1,4,9] As such, high pressure and high temperature[10] metal reactors are typically required.

However, unlike St or MMA CRPs, which can be sampled conveniently from Schlenk reaction tubes on a gram scale, diene kinetics are challenging experimentally and imply multiple one data point experiments. As a result, unlike with the vast CRP literature on liquid monomers,[4–7] there is very little data on dienes, and most of it pertains to the higher boiling thus more convenient, ISO. Example include CRPs mediated by nitroxides,[11] RAFT agents,[12] Te,[13] iodine degenerative transfer (IDT) telomerizations,[14] and Co selective dimerizations.[15] Here, our earlier work on the Cp$_2$TiCl[16–18] organometallic mediated reversible deactivation (OMRP),[19] CRPs of BD,[16] ISO,[17] and DMBD[18] initiated by the radical ring opening of epoxides,[20] SET reduction of aldehydes[21] and halides[22] remain the sole examples of transition metal mediated[5] CRPs of dienes and of the synthesis diene block copolymers.[17] However, while successful, the Ti-mediated CRP remains a water-sensitive, organometallic protocol.[23,24]

The advantages of ATRP[4–7] (simplicity, inexpensive available reagents, catalytic nature, rational ligand fine-tuning, water tolerance etc.),[4–7] vs. all other typical CRP methods and those of emulsion (lower cost, water media, high rate)[1] vs. coordination/anionic polymerizations, suggest that emulsion ATRP is quite suitable for industrial scale-up. However, over 20 years and more than 10 000[7] articles since the inception of ATRP,[25] although the mechanistic understanding[4–7,26] has considerably developed for St and (meth)acrylates,[4–7] its extension to more reactive (vinyl acetate (VAc),[27] vinylidene fluoride (VDF),[28] ethylene) and as well as less reactive monomers such as dienes remains challenging. To date, the few earlier diene-ATRP efforts,[29] remain qualitative, without evidence of M_n control, and missing specific details on the mechanism, kinetics, effect of reaction parameters, and especially on the complex correlation of the side reactions with the polymerization variables.

To address this, we set up a research program intended to provide an in-depth, quantitative evaluation of the scope and limitations of diene-ATRP, towards the synthesis of complex dienes architectures.[30] After preliminary studies on CuX initiated diene free radical polymerizations,[31] we subsequently demonstrated[30] that although the failure of diene-ATRP was blamed on BD/CuX catalyst coordination,[7,32] this has little bearing on the polymerization outcome. Thus, by contrast to polar AN,[33] the weak coordination[34] of St, MA or MMA[35] to Cu(I)X complexes with open coordination sphere does not interfere with the corresponding ATRPs. Moreover, CuX-μ-(1,3-Diene)-CuX[36] complexes can be prepared only below $T < -78$ °C. As such, 1,3-dienes are poor Lewis bases, and vastly inferior to typical Cu N- or P-ligands at the relatively high temperatures ($T > 100$ °C) of BD-ATRP. In reality, the culprit is the weak primary 1,4 P$_n$–CH$_2$–CH=CH–CH$_2$–X or secondary 1,2 P$_n$–CH$_2$–CH(CH=CH$_2$)–X allylic halide chain ends, and BD-ATRP fails predominantly via decrease of its halide chain end functionality (CEF) with conversion.

As a results of the P$_n$–X bond dissociation energy (BDE) order of allyl < AN < MMA < St < MA < VAc < VDF < Et,[32] the allyl–X termini are the weakest polymer chain ends, regardless of the X CRP agent[37] and consequently, the weakest of all ATRP halide chain ends[9] (BDE$_{25C}^{Allyl-Cl}$ = 71.3 kcal mol^{-1}, BDE$_{25C}^{Allyl-Br}$ = 56.7 kcal mol^{-1}).[32]

While there is very little data on the ATRP parameters of allyl halides ($k_{actCuBr,PMDETA}^{Allyl-Br,20C}$ = 3.8 × 10^{-2} L mol^{-1} s^{-1},[38] $k_{actCuX,Me6TREN}^{Allyl-Br,25C}$ = 3.26 × 10^2 L mol^{-1} s^{-1},[39] $K_{ATRPCuBr,bpy}^{Allyl-Br,22C}$ = 3 × 10^{-9},[40] $K_{ATRPCuBr,TPMA}^{Allyl-Br,22C}$ = 1.7 × 10^{-5},[6,40] $K_{ATRPCuCl,TPMA}^{Allyl-Cl,22C}$ = 2.3 × 10^{-6} (ref. 40)), they do suggested that polybutadiene halide chain ends (PBD-X) and their corresponding propagating allyl radicals (PBD$^·$) likely have highest of k_{act} and lowest k_{deact} values of all[4–7] typical ATRP monomers. As a result, dienes would exhibit the largest reversible dissociation equilibrium constants in CRPs mediated by the persistent radical effect ($K_{ATRP}^{Allyl-Br}/K_{ATRP}^{CH_3CH(CN)-Br}/K_{ATRP}^{(CH_3)_2C(COOCH_3)-Br}/K_{ATRP}^{CH_3CH(Ph)-Br}/K_{ATRP}^{CH_3CH(COOCH_3)-Br}$ = 890/730/28/6/1, 90 °C, i.e. BD > AN > MMA > St > MA),[32] and the fastest exchange rates in CRPs mediated by degenerative transfer (DT).

On the downside, facile PBD-X activation but slow PBD$^·$ deactivation allows competing processes to decrease halide CEF and broaden the PDI.[4–7] As such, our study on the effect of the initiator, halide, catalyst, ligand, solvent, temperature and ATRP method indicated[30] that besides a low b_p, DA monomer dimerization,[8] very low k_p,[9] allyl chain transfer and typical termination by recombination,[41] the allyl PBD-X/PBD$^·$ are the most susceptible all ATRP chain ends to side reactions such as β-H eliminations,[42] CuX/CuX$_2$/L oxidations/reductions[5,43] or catalytic termination[44] of propagating radicals and correspondingly, to thermal or base catalyzed PBD-X dehydrohalogenation by quaternization[45] with nucleophilic/basic N- or P-ligands in basic/polar solvents, followed by thermal onium elimination/fragmentations[46] which are driven by the formation of terminal allenes or conjugated double bonds. Therefore, catalytic solution ATRP procedures particularly ICAR with tertiary Br > Cl ester initiators in apolar solvents (toluene) are preferred since they employ much less of a potentially nucleophilic ligand (bpy or MeO-bpy vs. alkyl polyamines) and afford poly(butadiene) (PBD) with reasonably high Br chain end functionality (Br-CEF) suitable for the synthesis PBD block copolymers.

However, in addition to the well-studied Cu systems, other transition metals with variety of ligand types mediate ATRP. Some of the other more effective ones for styrene and (meth)acrylates are based on group 8 and group 10 complexes, especially Fe[5,47] and are worth exploring for dienes as well. We have recently investigated Ni, Pd and Pt complexes[30c] and we are extending our studies below to iron.

Experimental

Materials

2,2′-Bipyridiyl (bpy, 99%), iron(II) phthalocyanine (FePC, 95%), Dibenzo-18-crown-6 (DB18C6, 98%) from Alfa Aesar, tetrabutylammonium bromide (Bu$_4$NBr, 99%) from Acros, 1,4,7,10,13-pentaoxacyclopentadecane (15C5, 98%) from Ark Pharm, tetra-

hydrofuran (THF, 99.9%) HPLC grade from Fisher, bis(cyclo-pentadienyl)iron(II) (Cp$_2$Fe, 99%), 1,1′-bis(diphenylphosphino) ferrocene (DPPF, FeCp(PPh$_2$)$_2$), iron pentacarbonyl (Fe(CO)$_5$, 99.5%) all from Strem Chemicals, iron(II) chloride tetrahydrate (FeCl$_2$, 99%), iron(III) chloride hexahydrate (FeCl$_3$, 98%), iron(II) bromide (FeBr$_2$, 98%), iron(III) bromide (FeBr$_3$, 98%), 4-4′-dimethoxy-2-2′-bipyridine (MeO-bpy, 97%), $N,N,N′,N″,N″$-penta-methyldiethylenetriamine (PMDETA, 98%), 1,10-phenanthro-line (Phen, 99%), toluene anhydrous (99.9%), 1,4,7,10-tetraoxa-cyclododecane (12C4, 98%), tetrabutylammonium chloride (Bu$_4$NCl, 97%), tetrabutylphosphonium bromide (Bu$_4$PBr, 98%), tetrabutylammonium iodide (Bu$_4$NI, 99%), tris(2,4,6-tri-methoxyphenyl) phosphine (TTMPP), Tri-$tert$-butylphosphine (P(t-Bu)$_3$, 98%), Tri-n-butylphosphine (P(n-Bu)$_3$, 98%), Tris(per-fluorophenyl)phosphine (97%), Tris(4-trifluoromethylphenyl) phosphine (97%), triphenylphosphine (TPP, 99%), ethyl 2-bromo-isobutyrate (EBiB), 1,3-butadiene (BD, 99%) all from Sigma-Aldrich, were used as received. 1,1′-biphenylyl-1,4-bis(2-bromo-propanoate) (Br–C(CH$_3$)$_2$–CO–O–C$_6$H$_4$–C$_6$H$_4$–O–CO–C(CH$_3$)$_2$–Br, DB3) was synthesized as previously described.[30] DAMAR H25SL/Black light bulb from Lightbulb Depot (365 nm, 6 mW cm^{-2}) and blue 5050 LED strip light (1 m strip, λ = 450 nm, 4 mW cm^{-2}) from Solid Apollo LED were used for photo-mediated experiments.

Techniques

^{1}H NMR (500 MHz) spectra were obtained on a Bruker DRX-500 at 24° C in chloroform-d. Gel Permeation Chromatography (GPC) was performed on a Waters GPC system equipped with a PL-ELS1000 evaporative light scatter-ing (ELS) detector and a Jordi mixed bed two columns setup at 40 °C. THF (Fisher, 99.9% HPLC grade) was used as eluent at a flow rate of 1 mL min^{-1}. Number-average (M_n) and weight-average molecular weights (M_w) were determined from cali-bration plots constructed with PS standards. Since low M_n polydienes are quite soluble, precipitation in MeOH artificially lowers PDI, and we are reporting herein the values of raw samples. As seen for the Te-CRP[13] of isoprene, PSt calibrated GPC overestimates M_n. Thus, the initiator efficiency (IE = M_n^{theor}/M_n^{GPC}) values are underestimated.

Butadiene polymerization

As we have previously shown for the low boiling VDF[28] as well as for the Cp$_2$TiCl$_2$-mediated[16–18] diene OMRPs, the current BD-ATRPs were not performed in metal reactors, but rather in low pressure glass tubes that enable faster optimization and reproducible sampling under Ar after cooling the tube with dry ice/acetone to prevent BD evaporation.

In a typical N-ATRP procedure, FeCl$_3$·6H$_2$O, (0.1917 g, 0.71 mmol), TTMPP (0.567 g, 1.06 mmol) and toluene (3 mL) were added to a 35 mL Ace Glass pressure tube, which was purged with Ar, and cooled to ~−80 °C in a dry ice/acetone bath. DB3 (0.1719 g, 0.36 mmol) was then added. BD (1.92 g, 36 mmol) was condensed on top of the frozen reaction mixture which was then degassed by a series of vacuum/Ar refill cycles. The tube was placed in an oil bath at 110 °C.

Sampling was performed under Ar, after cooling in a dry ice/acetone bath, and the system was degassed after each sampling. For photopolymerizations, the light source was placed in the bath next to the tube.

The monomer conversion was determined by integrating the alkene resonances of the polymer $vs.$ the methyl resonance of toluene, which was used both as internal standard and solvent. The halide (Cl, Br) chain end functionality (CEF) was calculated by integrating the allyl Br or Cl resonances at $\delta \sim 4$ ppm $vs.$ the alkoxy resonance of EBIB at $\delta \sim 4.2$ ppm or $vs.$ the aromatic DB3 resonances at $\delta \sim 7.1$ or 7.6 ppm.

Results and discussion

Initial considerations

Widely used in organic and organometallic transformations,[48] Group 8 metals are likely the second most studied and pre-ferred class of transition metal ATRP catalysts besides Cu.[5] Indeed, a wide variety of N-, P-, C-, O-, S-, Cl and Br ligated Fe, Ru and Os complexes are successful in the ATRP of styrenes and (meth)acrylates,[5,47] and were also tested for vinyl chlo-ride[49] or vinylidene fluoride.[28] The abundant Fe offers the additional advantages of wide availability, lower cost, as well as biocompatibility and was studied with a variety of stoichio-metric and catalytic ATRP protocols[47] including ICAR or ARGET, as well as initiator-free or ligand-free systems or photo[50]-ATRP. In the later cases, initiation occurs following $in\ situ$ 1,2-halogenation of the monomer double bond in the dark, or by radical addition of X$^•$ derived from FeX$_3$ photolysis, and where strongly reducing phosphine ligands such as P[Ph(2,4,6-MeO)$_3$]$_3$[51] (TTMPP) act as $in\ situ$ ARGET-like redu-cing agents for FeX$_3$.

However, a clear comparison between Fe and Cu under similar conditions is not available, and while the halide, ligand and solvent are very important polymerization para-meters which affect the K_{ATRP} of Cu mediated ATRP of St and (meth)acrylates, across 6–7 orders of magnitude,[4–7] quantitat-ive k_{act}, k_{deact} or K_{ATRP} data for Fe remain limited primarily to high pressure Fe-ATRP,[52] or to ammonium halide,[53] TTMPP[54] or porphyrin[55] ligands, and the rational ranking of solvents, ligands and Cl $vs.$ Br systems is lagging far behind the Cu systems.

While one may expect dienes to broadly parallel the slowly propagating St in ATRP behavior, such trends are likely masked by high tendency of the weak allyl halide chain ends to undergo side reactions such as basic solvent catalyzed dehydrohalogenations or quaternizations with nucleophilic ligands, as well as by catalyst mediated oxidations/reductions and terminations of the propagating radical.[43,44] In addition, unlike the case of Cu mediated ATRP where diene coordi-nation is poor,[36] both Fe and Ru neutral or cationic diene complexes ($e.g.$ Fe/Ru(0)(CO)$_3$(η_4-C$_4$H$_6$))[56] are somewhat stable. Thus, while the $in\ situ$ formation of BD complexes with Fe or Ru halides in the presence of the better ligating phosphines or amines is unlikely at the high ($T > 100$ °C) ATRP temperatures,

transient coordination remains possible and may influence the polymerization outcome.

The structures of the iron complexes tested in this work (Chart 1) include various FeX$_2$/L and FeX$_3$/L combinations where X = Cl, Br and L = bpy, MeO-bpy, PMDETA, Phen, Bu$_4$NCl, Bu$_4$NBr, Bu$_4$PBr, Bu$_4$NI, 12C4, 15C5, DB-18C6, PPh$_3$ and P(C$_6$H$_2$(OMe)$_3$)$_3$, and well-defined complexes such as Fe(CO)$_5$, Cp$_2$Fe(CO)$_4$, FeCp$_2$, Fe(CpPPh$_2$)$_2$ and FePC (phthalocyanine), as well as ligand-free or initiator-free experiments in the dark or under irradiation. Here, due to the TBPO, ligand or light assisted reduction of FeX$_3$ or interconversion (con/disproportionation) of various oxidation states, the starting valence of the metal may not be essential. The results are summarized in Table 1 and Fig. 1–11, and the mechanism is illustrated in Scheme 1.

Butadiene initiation produces relatively less reactive, allyl delocalized PBD$^•$ radicals. Thus, it occurs easily from all typical alkyl halide ATRP initiators,[16–18,30] which all provide more reactive radicals.[32] As our earlier studies with Cu indicated a clear Br ≫ Cl preference,[30] the R–Br tertiary bromoester initiators used here are the typical Ebib and a difunctional analog, DB3, but a comparison with α,α-dichloro-p-xylene (DCPX) is also included. While in ICAR-ATRP the halide chain end is predominantly (>90%)[5] derived from the initiator, a halide exchange process is expected in stoichiometric N-ATRP systems.

A typical ^{1}H NMR of polybutadiene (PBD) prepared by Fe-mediated ATRP is presented in Fig. 1 and demonstrates the initiation by DB3 (aromatic resonances at $\delta \sim$ 7–7.5 ppm), the polymerization by a halide atom transfer (allyl Br/Cl chain ends, $\delta \sim$ 4–4.5 ppm, which also allow the calculation of the halide chain end functionality, Cl/Br-CEF), and the free radical nature of the polymerization (by the classic[1] ~80/20 free
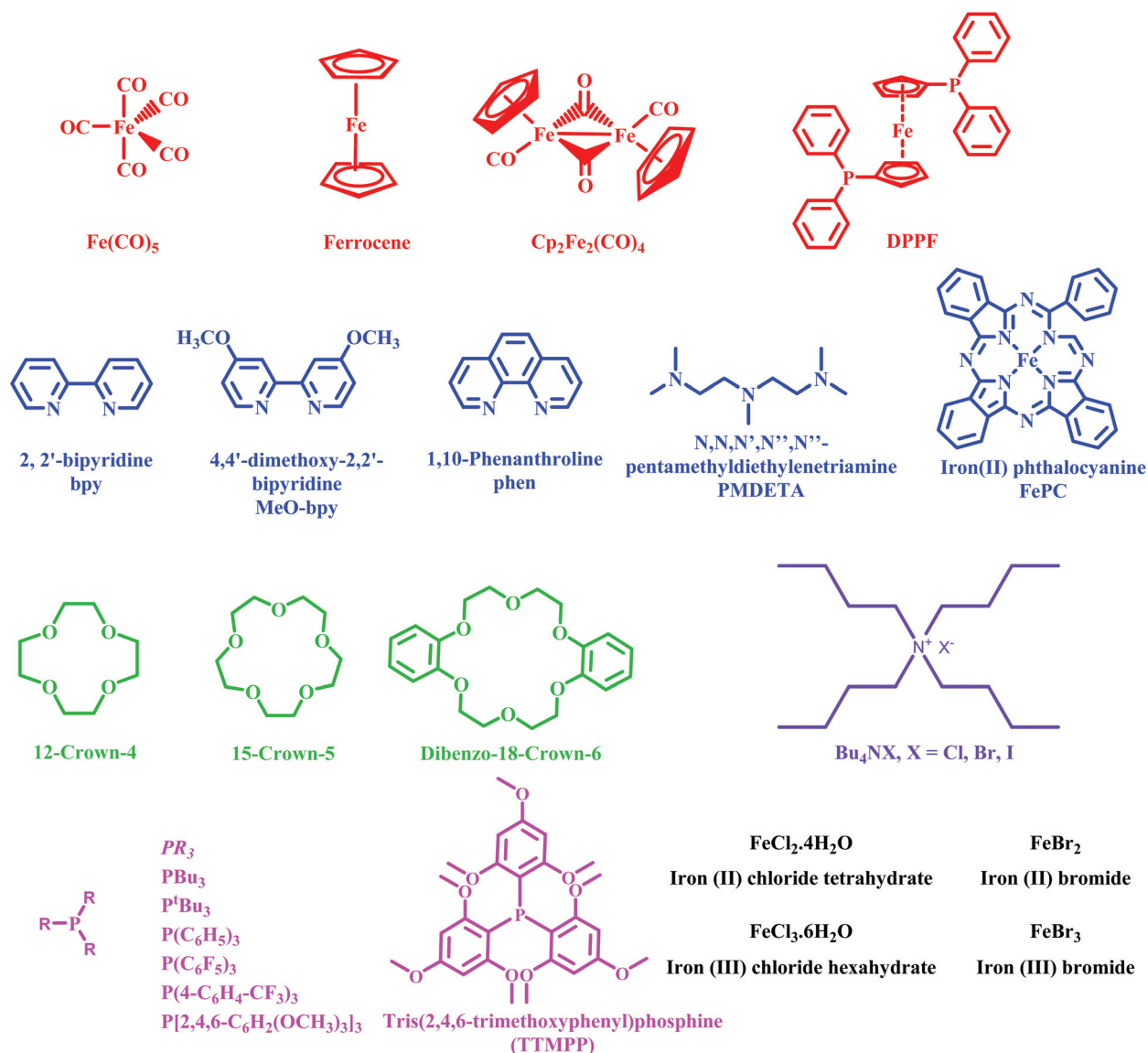

Chart 1 Ligands and Fe complexes tested in BD-ATRP.

Polymer Chemistry

Table 1 Fe Mediated BD-ATRP

Exp	Cat/L	[TBPO]/[Cat]/[L]	M_n	PDI	I.E. & $M_n^0 \times 10^{-3}$	Time (h)	Conv (%)	$k_p^{app} \times 10^3$, h^{-1}	X-CEF, %
1	Cp$_2$Fe[a]	0.20/0.15/0.00	77 300	1.44	0.01/42	120	15	1.3	0
2	Cp$_2$Fe[b]	0.00/0.50/0.00	11 300	1.57	0.01/35	144	10	0.8	0
3	(Ph$_2$P-Cp)[b]	0.20/0.05/0.00	2900	1.64	0.45/2.4	144	16	1.6	85
4	(Ph$_2$P-Cp)[b]	0.00/0.20/0.00	4000	1.17	0.30/0.42	144	13	1.3	75
5	Fe(CO)$_5$[b]	0.20/0.10/0.00	33 000	1.53	0.05/26	96	19	2.2	13
6	Cp$_2$Fe$_2$(CO)$_4$[b]	0.20/0.05/0.00	25 000	1.69	0.07/9.4	120	22	2.2	14
7	Cp$_2$Fe$_2$(CO)$_4$[b,c]	0.00/0.10/0.00	1970	1.50	0.45/0.46	54	6	2.4	29
8	Cp$_2$Fe$_2$(CO)$_4$[b,c]	0.00/1.00/0.00	16 320	1.71	0.07/9.66	60	16	2.4	0
9	FeBr$_2$/Phen[b]	0.20/0.05/0.15	36 000	1.52	0.03/18	144	10	0.7	0
10	FeBr$_3$/Phen[b]	0.20/0.05/0.15	49 700	1.48	0.03/41	144	16	1.2	0
11	FeBr$_2$/bpy[b]	0.00/2.00/4.00	40 200	1.46	0.05/0.43	96	15	1.7	11
12	FeBr$_2$/MeO-bpy[a]	0.20/0.05/0.15	79 100	1.61	0.02/23	96	25	3.0	0
13	FeBr$_2$/MeO-bpy[b]	0.00/2.00/4.00	37 700	1.81	0.03/0.47	96	11	1.2	5
14	FeBr$_3$/MeO-bpy[b]	0.20/0.05/0.15	32 800	1.50	0.05/0.48	96	15	2.0	5
15	FePC[a]	0.20/0.15/0.00	45 000	2.11	0.03/2.7	144	20	2.0	47
16	FePC[b]	0.00/0.50/0.00	750	1.05	—/—	144	0	0.0	0
17	FeCl$_3$/PMDETA[b]	0.20/0.05/0.15	32 000	1.56	0.09/10	196	46	3.0	12
18	FeBr$_2$/PMDETA[b]	0.20/0.05/0.15	26 400	1.62	0.09/21	144	36	3.0	18
19	FeBr$_2$/Bu$_4$NCl[b]	0.00/2.00/3.00	4170	1.18	0.33/1.3	144	17	0.4	69
20	FeBr$_2$/Bu$_4$NBr[b]	0.00/2.00/3.00	2380	1.25	0.32/1.5	144	5	0.2	51
21	FeBr$_2$/Bu$_4$NI[b]	0.00/2.00/3.00	3560	1.33	0.22/1.8	144	5	0.2	53
22	FeBr$_2$/Bu$_4$PBr[b]	0.00/2.00/3.00	1100	1.06	0.27/0.92	144	6	0.4	21
23	FeBr$_3$/Bu$_4$NCl[b]	0.20/0.05/0.15	5850	1.58	0.17/1.8	144	9	0.7	41
24	FeBr$_3$/Bu$_4$NBr[b]	0.20/0.05/0.15	12 100	1.38	0.05/8.6	144	3	0.7	25
25	FeBr$_3$/Bu$_4$NCl[b,c]	0.00/0.05/0.15	10 900	1.95	0.35/0.52	100	61	10	57
26	FeCl$_3$/Bu$_4$NCl[b]	0.20/0.05/0.15	3590	1.26	0.39/1.1	120	17	1.2	13
27	FeCl$_3$/Bu$_4$NBr[b]	0.20/0.05/0.15	5190	1.42	0.22/4.5	120	12	1.3	11
28	FeCl$_3$/Bu$_4$NCl[b,c]	0.00/0.05/0.15	9900	1.95	0.39/5.5	120	63	10	60
29	FeBr$_2$/12C4[b]	0.00/2.00/3.00	670	1.04	—/—	60	4	—	0
30	FeBr$_3$/12C4[b]	0.20/0.05/0.15	7940	1.56	0.16/4.7	144	15	0.5	35
31	FeBr$_3$/15C5[b]	0.20/0.05/0.15	4310	1.40	0.30/2.1	144	10	0.2	42
32	FeCl$_2$/12C4[b]	0.00/2.00/3.00	540	1.04	—/—	60	2	—	0
33	FeCl$_3$/12C4[b]	0.20/0.05/0.15	7510	1.57	0.27/1.8	80	28	4.2	22
34	FeCl$_3$/15C5[b]	0.20/0.05/0.15	30 200	1.68	0.05/5.3	144	17	1.4	19
35	FeCl$_3$/DB18C6[b]	0.20/0.05/0.15	40 500	1.75	0.05/6.9	124	25	2.1	14
36	FeCl$_3$/P(C$_6$F$_5$)$_3$[b]	0.00/2.00/3.00	920	1.07	—/—	96	0	—	0
37	FeCl$_3$/P[Ph(4-CF$_3$)]$_3$[b]	0.00/2.00/3.00	870	1.07	—/—	96	0	—	0
38	FeCl$_3$/PPh$_3$[b]	0.00/2.00/3.00	700	1.03	—/—	96	0	—	0
39	FeCl$_3$/PPh$_3$[b]	0.20/2.00/3.00	1690	1.2	0.60/0.32	96	11	0.6	83
40	FeBr$_3$/PPh$_3$[b]	0.00/2.00/3.00	840	1.06	—/—	96	0	—	0
41	FeBr$_3$/PPh$_3$[b]	0.20/2.00/3.00	890	1.04	0.64/0.73	96	2	0.2	33
42	FeCl$_3$/P(n-Bu)$_3$[b]	0.00/2.00/3.00	840	1.06	—/—	96	0	—	0
43	FeCl$_3$/P(t-Bu)$_3$[b]	0.00/2.00/3.00	2771	1.16	0.44/0.32	96	10	1.0	76
44	none/TTMPP[b]	0.00/0.00/2.00	98 100	1.48	0.01/82	72	3	0.4	0
45	FeBr$_2$/TTMPP[b]	0.00/2.00/3.00	108 300	2.30	0.01/71	120	11	0.9	40
46	FeBr$_3$/TTMPP[b]	0.00/2.00/3.00	18 500	1.20	0.10/2.5	72	19	4.1	45
47	FeBr$_3$/TTMPP[b]	0.20/0.05/0.15	2200	1.41	0.55/1.2	144	13	1.1	66
48	FeBr$_3$/TTMPP[b]	0.00/0.05/0.15	1560	1.06	0.46/0.34	96	4	0.4	33
49	FeBr$_3$/TTMPP[b,c]	0.00/0.05/0.15	7300	1.31	0.42/0.28	96	48	7.0	87
50	FeCl$_2$/TTMPP[b]	0.00/2.00/3.00	17 700	1.14	0.06/0.73	76	11	1.6	50
51	FeCl$_3$/TTMPP[b]	0.00/2.00/3.00	19 700	1.18	0.20/2.1	150	46	4.1	63
52	FeCl$_3$/TTMPP[b]	0.00/2.00/3.00	11 070	1.14	0.20/0.2	92	32	4.1	65
53	FeCl$_3$/TTMPP[b]	0.00/0.05/0.15	1830	1.14	0.41/0.46	96	5	0.5	35
54	FeCl$_3$/TTMPP[b]	0.20/0.05/0.15	4030	1.57	0.44/0.15	144	24	1.9	72
51	FeCl$_3$/TTMPP[b,c]	0.00/0.05/0.15	9920	1.41	0.41/0.89	144	66	7.8	88
52	FeCl$_3$/TTMPP[d]	0.00/2.00/3.00	8800	1.46	0.14/3.9	48	13	3.0	60
53	FeBr$_3$[c]	0.00/1.00/0.00	25 900	2.24	0.12/14	160	49	4.6	21
54	FeBr$_3$[e]	0.00/1.00/0.00	11 600	1.64	0.23/3.8	96	41	5.9	17
55	FeBr$_3$[b,c]	1.00/0.05/0.00	39 200	1.82	0.07/7.0	96	39	5.7	31
56	FeCl$_3$[b]	0.00/1.00/0.00	900	1.06	—/—	72	—/—	—	—
57	FeCl$_3$[c]	0.00/1.00/0.00	22 900	1.57	0.17/2.0	160	64	6.6	23
58	FeCl$_3$[e]	0.00/1.00/0.00	28 000	1.68	0.15/2.8	144	69	7.9	31
59	FeCl$_3$[b,c]	1.00/0.05/0.00	5800	2.28	0.40/2.9	120	35	4.0	51

All reaction ratios [BD]/[R–X] = 100/1. [a] EBIB. [b] DB3. [c] BLB irradiation. [d] DCPX. [e] Blue-LED irradiation in toluene at T 110 °C, $M_n^0 = M_n$ intercept at zero conversion. k_p^{app} = initial apparent rate constant
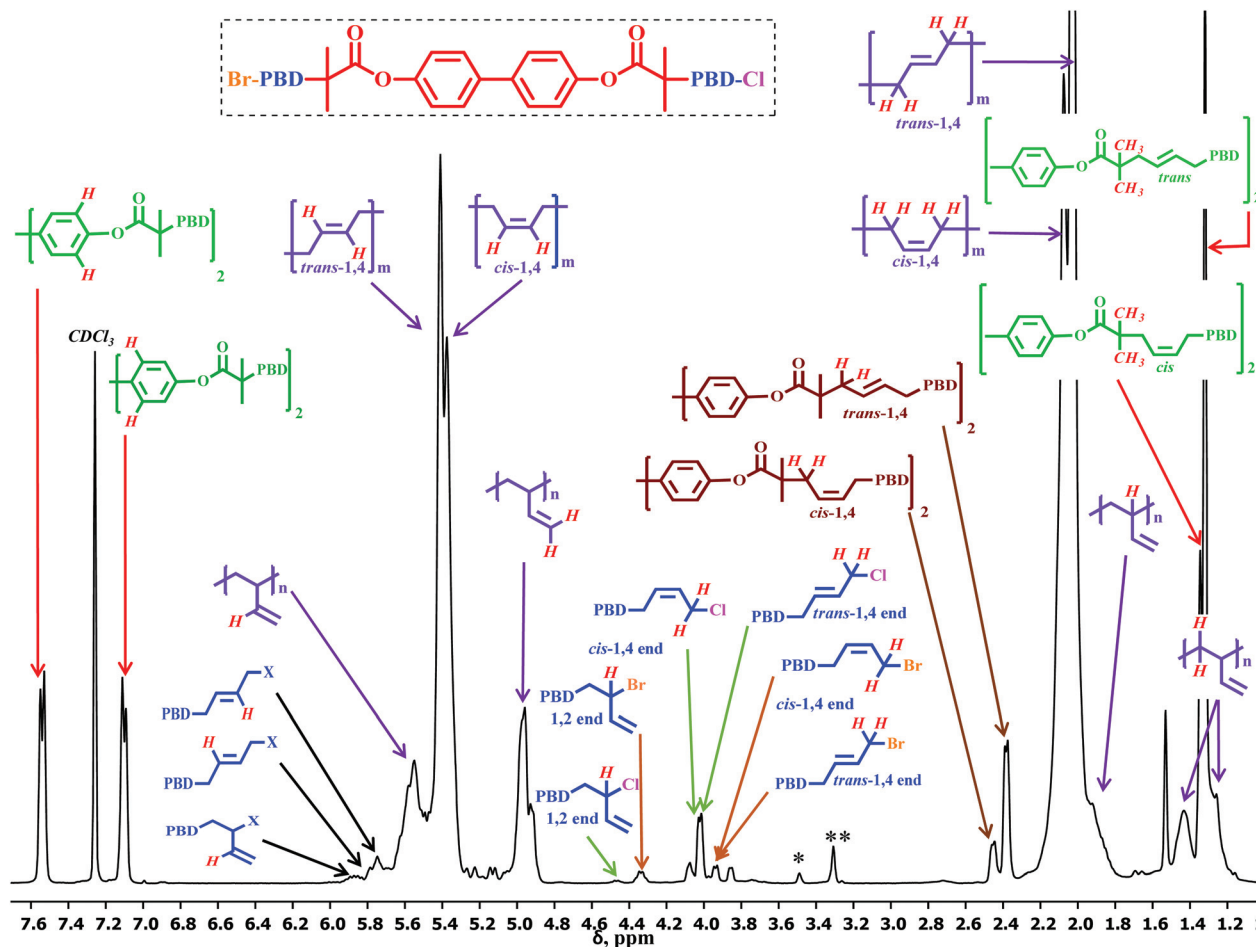
Fig. 1 ^{1}H NMR of PBD from [BD]/[DB3]/[FeCl$_3$·6H$_2$O]/[TTMPP] = 50/1/2/3. M_n = 6334, PDI = 1.15, X-CEF = 0.63. *TTMPP, **MeOH.

radical distribution of the 1,4 and 1,2-BD isomeric main chain units).

While the values of k_{act} for most of these metal complexes and R–Br are not known, for good polymerization control and narrow PDI, it is desirable that initiation is faster than propagation. This aspect is also relevant in the Br/Cl-CEF calculation from the integration of the ally Br/Cl chain ends *vs.* initiator resonances. For Ebib, the kinetics of initiator activation can be measured due to the different positions of the CH$_3$–*CH$_2$*–O– signal in the starting Br initiator ($\delta \sim 4.2$ ppm) *vs.* in the chain

end ($\delta \sim 4.1$ ppm), and are shown in some instances. Unfortunately, the aromatic DB3 resonances are indistinguishable in the starting and polymer-bound initiator. Here, the R–*CH$_2$*–CH=CH–CH$_2$– connectivity at $\delta \sim 2.5$ ppm could be used, but it overlaps with the CH$_3$ resonance of toluene, which is used as reference for BD conversion determination. As such, the Br/Cl-CEF values of unprecipitated, DB3 initiated PBD may be underestimated if the initiation is slow.

The polymerizations were carried out at 110 °C where <10% of the monomer dimerizes by thermal Diels–Alder cyclo-addition,[30] and where the half lifetime of TBPO enables a continuous radical supply in ICAR for over a week.[1,57] The apolar toluene was used as a solvent to minimize base-catalyzed thermal dehydrohalogenation, halide chain end alkylations/quaternizations and other side reactions. While FeBr$_2$ and other Fe complexes were shown to mediate ATRP even in the absence of ligands,[58] such polymerizations were only shown for polar monomers (*e.g.* acrylates) in polar solvents (*e.g.* ACN) which help solubilize FeBr$_2$. Thus, for toluene, ligands are likely needed, even if some diene/FeX$_3$ coordination occurs. As excess ligand may alkylate the weak PBD-X chain ends,[30] typical R-X/cat = 1/1 stoichiometric N-ATRP ratios were not always tested, but comparisons of pseudo N-ATRP with low
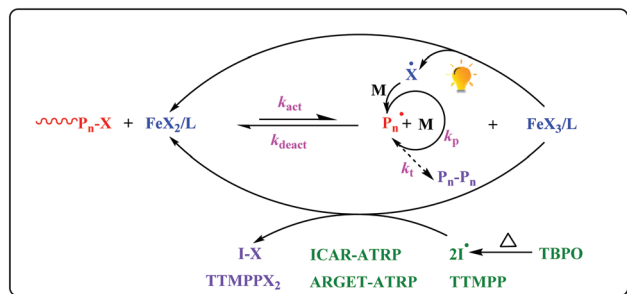
Scheme 1 Mechanism of Fe-mediated BD-ATRP.

ratios and ICAR (*e.g.* [BD]/[RBr]/[TBPO]/[Mt] = 100/1/0/0.2 *vs.* 100/1/0.2/0.05 or 100/1/0.2/0.2) are provided in a few cases and illustrate the beneficial effect of TBPO, TTMPP or light.

C-Ligands: Fe(CO)$_5$, Cp$_2$Fe, (Ph$_2$PCp)$_2$Fe, Cp$_2$Fe$_2$(CO)$_4$ and photo-ATRP

By contrast to *in situ* generated FeX$_n$/L complexes where the nucleophilic ligand may react with the PBD-X chain ends, well-defined Fe complexes with C-ligands are not expected to dissociate L, and are thus of interest in BD-ATRP. A comparison of all ligands was performed in ICAR, while Cp$_2$Fe and (Ph$_2$PCp)$_2$Fe were also tested in N-ATRP.

However, in all cases (Fig. 2), the polymerizations only proceed to <20%. For the Fe(II) species, in both ICAR and pseudo N-ATRP, Cp$_2$Fe presents some dependence of M_n on conversion, but with a high M_n intercept ($M_n^0 \sim 40\,000$), and with ICAR having a slightly better initiator efficiency, lower PDI (1.44 *vs.* 1.57) and faster rate ($k_p^{app} = 1.3 \times 10^{-3}$ h^{-1} *vs.* 8×10^{-4} h^{-1}), than pseudo N-ATRP. However, both polymers are devoid of halide chain end functionality (Br-CEF). This is consistent with the kinetics of Ebib activation which reveal that only trace (~1%) Ebib reacted. The (Ph$_2$PCp)$_2$Fe mediated polymerization displays a minor dependence of M_n *vs.* conversion with an origin intercept, a much lower PDI of ~1.2 *vs.* 1.6 for pseudo N-ATRP *vs.* ICAR. However, while it exhibits a relatively high Br-CEF ~ 0.8 in both cases, and a fast initial rate ($k_p^{app} = 6 \times 10^{-3}$ h^{-1}), it then progresses very little, especially for ICAR.

An in-between behavior is seen for Fe(CO)$_5$ and Cp$_2$Fe$_2$(CO)$_4$, which present identically fast ICAR kinetics ($k_p^{app} = 2.2 \times 10^{-3}$ h^{-1}) and similarly low Br-CEF ~ 0.1. However, while Fe(CO)$_5$ has a relatively flat M_n profile with a high intercept ($M_n^0 \sim 26\,000$), Cp$_2$Fe$_2$(CO)$_4$ shows CRP features

with higher initial PDI, which converge to ~1.6 for both. Similar CRP features with lower initial PDIs and slightly faster rates are observed for Cp$_2$Fe$_2$(CO)$_4$ using N-ATRP conditions under black light bulb (BLB) irradiation, where the dimer splits to produce CpFe(CO)$_2$• which can also activate alkyl halides.[28h] However, a similar experiment with catalytic CpFe(CO)$_2$ only affords low (~5%) conversion. Thus, since (Ph$_2$PCp)$_2$Fe affords high CEF, but remains kinetically stagnant, the following Cp$_2$Fe$_2$(CO)$_4$ > Cp$_2$Fe > Fe(CO)$_5$ > (Ph$_2$PCp)$_2$Fe trend occurs in terms of ATRP control.

N ligands: bidentate (Bpy, MeO-bpy, Phen) and polydentate (PMDETA, PC) amines

A comparison of bpy *vs.* MeO-bpy is exemplified for N-ATRP with FeBr$_2$, whereas a comparison of MeO-bpy *vs.* Phen for both FeBr$_2$ and FeBr$_3$ is presented for ICAR in Fig. 3.

In N-ATRP, FeBr$_2$ affords a CRP with a linear dependence of M_n on conversion for both ligands. Here, consistent with the higher activity and nucleophilicity of MeO-bpy,[59] bpy affords better IE, lower initial PDI, higher Br-CEF (0.1 *vs.* 0.06) and slightly faster kinetics ($k_p^{app} = 1.7 \times 10^{-3}$ h^{-1} *vs.* 1.2×10^{-3} h^{-1}).

In ICAR, for both FeBr$_2$ and FeBr$_3$, MeO-bpy displays faster rates than phen (~3×10^{-3} *vs.* ~1×10^{-3} h^{-1}). For FeBr$_2$, both ligands show the same linear M_n *vs.* conversion trend with an intercept at ~20 000, but MeO-bpy proceeds to higher conversion (25% *vs.* 10%), and with higher initial PDI, which converges to 1.5 for both. However, only trace Ebib activation is observed. For FeBr$_3$, phen leads to an FRP behavior with an intercept at ~40 000 and no Br-CEF, while a clear M_n control (lower intercept and higher IE) is seen for MeO-bpy, with PDI ~ 1.5–1.6 and Br-CEF of ~0.07. Finally, the use of MeO-bpy in N-ATRP/FeBr$_2$ and ICAR/FeBr$_3$, shows M_n control
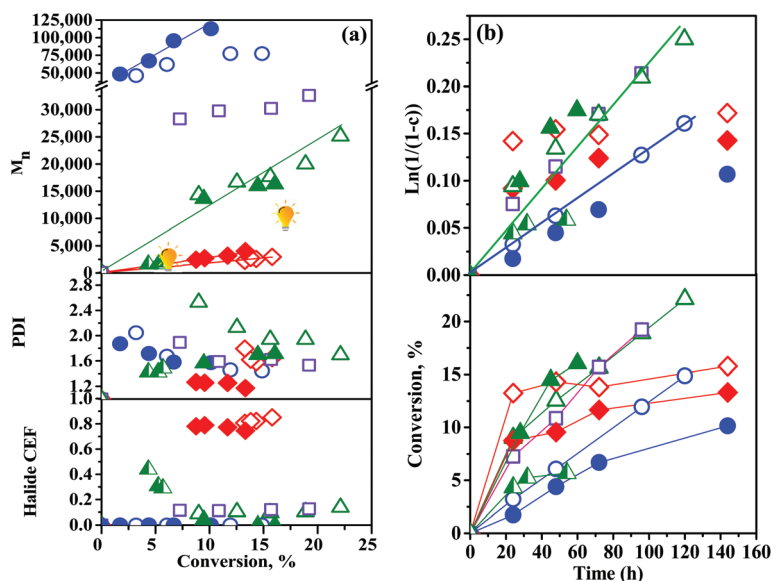

Fig. 2 Effect of Cp and CO ligands in BD-ATRP. (a) Dependence of M_n, PDI and Br-CEF on conversion, (b) kinetics. [BD]/[R−Br]/[TBPO]/[Fe] = 100/1/ X/Y. R−Br = EBiB, 0.2/0.15, Cp$_2$Fe (○); R−Br = DB3, X/Y = 0/0.5, Cp$_2$Fe (●); 0.2/0.05 or 0/0.2, (Ph$_2$PCp)$_2$Fe (◇, ◆); 0.2/0.1, Fe(CO)$_5$ (□); 0.2/0.05, Cp$_2$Fe$_2$CO$_4$ (△) and BLB irradiation: 0.0/0.1 and 0.0/1 Cp$_2$Fe$_2$CO$_4$ (▲, ▲).
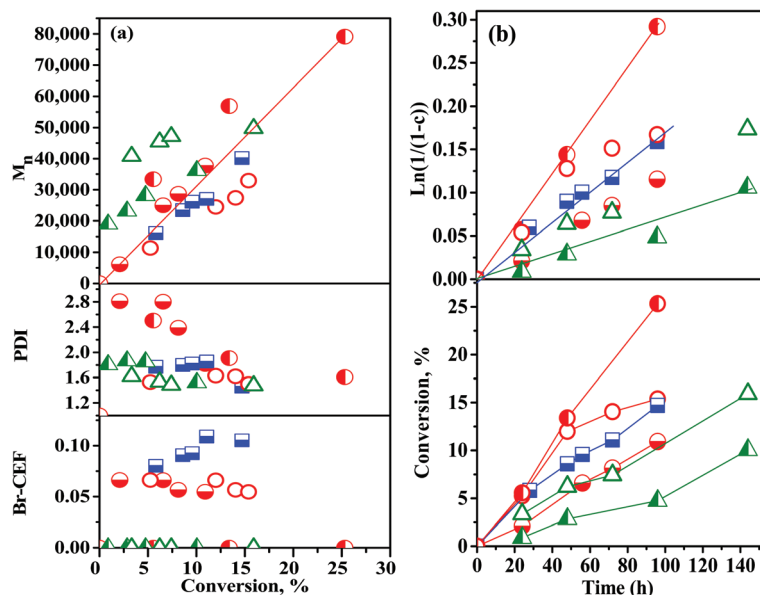
Fig. 3 FeBr$_2$ and FeBr$_3$ mediated N- and ICAR BD-ATRP with bidentate bpy, MeO-bpy and phen ligands, (a) dependence of M_n, PDI and Br-CEF on conversion, (b) kinetics. [BD]/[DB$_3$]/[**FeBr$_2$**]/[L] = 100/1/2/4, MeO-Bpy (◑), Bpy (▣); [BD]/[DB$_3$]/[TBPO]/[**FeBr$_2$** or **FeBr$_3$**]/[L] = 100/1/0.2/0.05/0.15, R−Br = Ebib, MeO-Bpy (◑, none); R−Br = DB$_3$, MeO-Bpy (none, ○), Phen (▲, △).
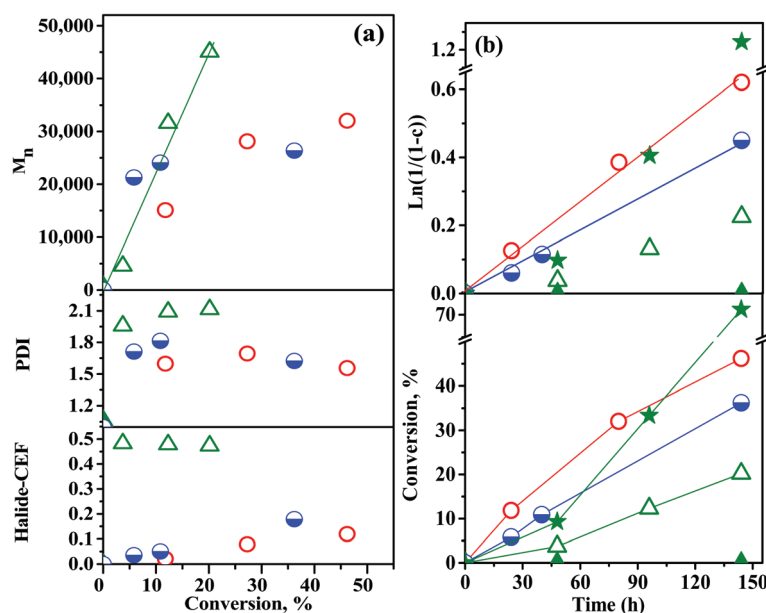
Fig. 4 Fe mediated BD-ATRP with multidentate PMDETA and phtalocyanine ligands, (a) dependence of M_n, PDI and Br-CEF on conversion, (b) kinetics. [BD]/[DB3]/[TBPO]/[**FeBr$_2$** or **FeCl$_3$**]/[PMDETA] = 100/1/0.2/0.05/0.15, (◑, ○); [BD]/[Ebib or DB3]/[TBPO]/[**FePC**] = 100/1/0.2/0.15 (△), 100/1/0/0.5 (▲) and Ebib activation (★).

in both, with similarly low Br-CEF ∼ 0.07, but with a better IE, lower PDI, and a faster rate for ICAR.

A comparison of multidentate N-ligands is provided by PMDETA with FeCl$_3$ and FeBr$_2$, and by iron phthalocyanine in Fig. 4. In ICAR, both FeCl$_3$ and FeBr$_2$ present identical kinetics (k_p^{app} ∼ 3 × 10^{-3} h^{-1}) where a better M_n *vs.* conversion trend is afforded by FeCl$_3$, while FeBr$_2$ shows marginally better Br-CEF of 0.18 *vs.* 0.1 and similar PDI ∼ 1.5.

Interestingly, while Fe[47] and various other metal porphyrins[60] were tested in the ATRP of St and MMA, where they may also enable an additional OMRP,[19] Fe phthalocyanins inhibited the OMRP of VAc.[61] Similarly, no polymerization is seen here for N-ATRP, but ICAR shows a clear linear dependence of M_n on conversion and PDI ∼ 2, and FePC is the only N-ligand that presents a high Br-CEF ∼ 0.5. This is consistent with a high and continuous activation of Ebib throughout the

polymerization (>70%, $k_{act}^{app} \sim 1.2 \times 10^{-2}$ h^{-1}), albeit with an induction time of >24 h for both Ebib and BD, but relatively fast thereafter ($k_p^{app} = 2 \times 10^{-3}$).

Thus, in view of the very low Br-CEF, and by contrast to Cu systems with the same ligands,[30] Fe/bidentate aromatic as well as polydentate aliphatic amines may not be suitable for good quality BD-ATRP. While in N-ATRP, amine chain end quaternization could be blamed for low Br-CEF, due to the lower catalyst/ligand amount, ICAR ATRP is expected to provide better Br-CEF and similar rate which should only be controlled by the TBPO amount.[4–7] However, while MeO-bpy, PMDETA and FePC display identical ICAR rates, phen is much slower, and the N-ATRP experiments are slower that the ICARs. Thus, the lack of Br-CEF, in conjunction with the low initiator efficiency of these systems indicate that similarly to their behavior in the ATRP of St and MMA,[62] FeX$_n$/N-ligands exhibit poor initiator and chain end halide activation, and as seen here, poor de-activation of allyl halides. By contrast, tetradentate aromatic cyclic systems appear far more promising, and although bpy was not tested in ICAR, the likely qualitatively sequence in terms of ATRP control is FePC > bpy > MeO-bpy > PMDETA ≥ Phen and FeCl$_3$ > FeBr$_2$.

Halide anions as ligands and photo-ATRP

Here, by contrast to typical MtX$_n$/L ATRP systems, the Fe "ligand" is in fact a halide, and the anionic metal complexes are counterbalanced by ammonium cations. Thus, such systems are not nucleophilic and should not alkylate the PBD-X chain ends. However, the additional halide from the ammonium salt[63] also affects the overall halide exchange process, and the mixed FeX$_{2,3}$/Bu$_4$NY (X, Y = Cl, Br, I) systems

afford a variety of Fe(II)X$_n$Y$_{4−n}$(NBu$_4$)$_2$, Fe(II)$_2$X$_n$Y$_{6−n}$(NBu$_4$)$_2$ or Fe(III)X$_n$Y$_{4−n}$(NBu$_4$), *etc.* derivatives with an ATRP reactivity dependent on halide composition.[63]

As such, due to the excess R–Br initiator, the initiator halide will always dominate in ICAR, with PBD-X and the Fe complexes equilibrating to predominantly Br. Indeed, for our R–Br/FeX$_n$/Bu$_4$NY (X = Cl, Br) ICAR ratios, the overall Cl mol fraction (*vs.* Br) for the FeCl$_3$/NBu$_4$Cl, FeBr$_3$/NBu$_4$Cl, FeCl$_3$/NBu$_4$Br and FeBr$_3$/NBu$_4$Br combinations is 0.15, 0.09, 0.06 and 0. By contrast, for stoichiometric N-ATRP, a variety of mixed halide complexes can be formed from the RBr/FeX$_{2,3}$/Bu$_4$NX = 2/(4,6)/3 mixtures, and for the combinations used here *i.e.* FeBr$_2$ with NBu$_4$Cl/Br/I, the Cl mole fractions are 0.33, 0 and 0.

Several trends are emerging in Fig. 5 below from ATRP comparisons of Bu$_4$NX (X = Cl, Br, I) and Bu$_4$PBr for FeBr$_2$, followed by the FeX$_3$/Bu$_4$NX (X = Cl, Br) combinations in ICAR, and finally by the effect of irradiation of a pseudo N-ATRP with Bu$_4$NCl, at the same ratios as ICAR, but in the absence of TBPO.

First, the comparison of all ammonium salts in N-ATRP with FeBr$_2$ reveals a clear Bu$_4$NCl ≫ Bu$_4$NBr > ∼Bu$_4$PBr > Bu$_4$NI trend with respect to polymerization control. Indeed, while all other reactions are trace polymerizations to <5% conversion, Bu$_4$NCl has a fast initial rate ($k_p^{app} \sim 5 \times 10^{-3}$ h^{-1}) to ∼20% conversion, but progresses little after the first sample. Nonetheless, it affords a remarkably high X-CEF ∼ 0.7 and PDI ∼ 1.2.

Likewise, the four FeX$_3$/Bu$_4$NX (X = Cl, Br) combinations of ICAR reconfirm the FeCl$_3$ > FeBr$_3$ and Bu$_4$NCl > Bu$_4$NBr above. Thus, while FeBr$_3$/Bu$_4$NBr barely affords trace (<4%) conversion, while FeCl$_3$ still affords ∼12% conversion, but as a FRP
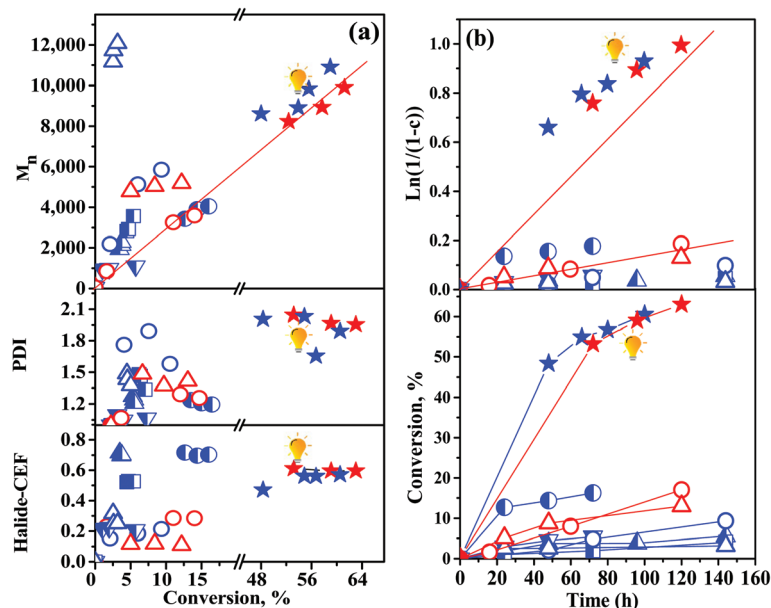

Fig. 5 Iron mediated BD–ATRP with halide ligands derived from Bu$_4$NCl, Bu$_4$NBr, Bu$_4$PBr, and Bu$_4$NI (a) Dependence of M_n, PDI and Br–CEF on conversion, (b) kinetics. [BD]/[DB3]/[**FeBr$_2$**]/[L] = 100/1/2/3: Bu$_4$NCl (◑), Bu$_4$NBr (△), Bu$_4$PBr (▽), Bu$_4$NI (▣); [BD]/[DB3]/[TBPO]/[**FeCl$_3$** or **FeBr$_3$**]/[L] = 100/1/0.2/0.05/0.15: Bu$_4$NCl (○, ○), Bu$_4$NBr (△, △), and 100/1/0.0/0.05/0.15, BLB irradiation, Bu$_4$NCl (★, ★).

with PDI ~ 1.5 and CEF ~ 0.1. By contrast, $FeCl_3/Bu_4NCl$ allows for narrower PDI (~1.3 vs. ~1.7), higher X-CEF (0.3 vs. ~0.2), twice the conversion, twice as fast vs. $FeBr_3/Bu_4NCl$ (i.e. 15% and 1.5×10^{-3} h^{-1} vs. 8% and 7×10^{-4} h^{-1}), and both present some elements of M_n control.

While no comparison exists for the same catalyst in both ICAR and ATRP, Bu_4NBr provides oligomers (<5% conversion) in both $FeBr_3$-ICAR and $FeBr_2$-ATRP, whereas Bu_4NCl gives 10–20% conversion and higher Br-CEF. Thus, for both $FeCl_3$ and $FeBr_3$, $Bu_4NCl \gg Bu_4NBr$ and for both Bu_4NCl and Bu_4NBr, $FeCl_3 \gg FeBr_3$, leading to $FeCl_3/Bu_4NCl > FeBr_3/Bu_4NCl > FeCl_3/Bu_4NBr \gg FeBr_3/Bu_4NBr$ trend in ATRP quality, which is consistent with the decrease in the Cl mole fraction above.

Finally, the effect of irradiation with a black light bulb (BLB) was also tested in photo-ATRP using the more successful Bu_4NCl with both $FeCl_3$ and $FeBr_3$ at ICAR ratios, but in the absence of TBPO. Here, FeX_3 photolyzes to FeX_2 and X[·] which can reinitiate the polymerization[50] (Scheme 1), and light serves as a reducing agent surrogate for ICAR. However, while high conversion could be promoted in ICAR by high TBPO levels, this would also lead to loss of control. By contrast, light mediated X-initiation affords a dormant allyl–X halide chain end, and is preferable to TBPO. Indeed, in both cases, the polymerizations show almost similar, linear M_n vs. conversion profiles, but proceed to much higher conversions (~60% vs. ~10–15%) with rates that are about ten times faster than the corresponding ICARs ($k_p^{app} = 1 \times 10^{-2}$ h^{-1} vs. ~ = 1×10^{-3} h^{-1}), and with much higher Br-CEF (~0.6 vs. 0.1), but also with broader PDI of ~2.

Crown ethers

Crown ethers are much less nucleophilic than amines, thus again of interest for BD-ATRP. While Fe/crown ether complexes such as $Fe(PF_6)_2/12C4^{64}$ and $FeCl_3 \cdot 6H_2O/(15C5$ or $18C6)^{65}$ are known, both 15C5 and 18C6 were only previously used as polymerization solvents (i.e. not in ligand amounts) in the Fe ATRP of MMA,[66] and there is no ATRP data on $FeCl_3 \cdot 6H_2O$ complexes with 12C4. Interestingly, water is still retained as a coordinating ligand in the crystal,[64,65] and although in terms of Lewis acidity, Fe(III) > Fe(II) and Cl > Br, it may dampen the Lewis acidity of $FeCl_3$ for all ligands, not only crown ethers.

Here, a comparison of 12C4, 15C5 and DB18C6 and that of 12C4 and 15C5 is provided in ICAR for $FeCl_3$ and respectively $FeBr_3$, whereas a $FeCl_2$ vs. $FeBr_2$ comparison is shown for 12C4 in N-ATRP in Fig. 6.

In ICAR with $FeCl_3$, all crown ethers enable CRPs with a linear dependence of M_n on conversion, but 12C4 affords better initiator efficiency, lower PDI (1.3–1.6 vs. 1.45–1.75) and twice faster rates ($k_p^{app} = 4.2 \times 10^{-3}$ vs. 2.1×10^{-3} h^{-1}) to higher conversions (~30%), than both 15C5 and DB18C6, which are very similar. While the Br-CEF values are relatively close (0.14–0.22), the 12C4 > 15C5 ≥ DB18C6 trend in polymerization control is still apparent. Likewise, for $FeBr_3$, although both polymerizations show much poorer control, and stop at ~10–15% conversion, 12C4 again affords ~ twice the conversion and the initial rate (3×10^{-3} vs. 1×10^{-3} h^{-1}) of 15C5. As seen for Bu_4NCl, while $FeBr_3$ does afford a better Br-CEF ~ 0.3, the M_n control is weak, and consistent with the nitrogen and halide ligands above, $FeCl_3$ again promotes faster, narrower and more controlled polymerizations than $FeBr_3$, for both 12C4 and 15C5.

By contrast, stoichiometric N-ATRPs with $FeCl_2$ or $FeBr_2$ and 12C4 lead only to trace polymerization in both cases. This may be due to either early irreversible termination and accumulation of FeX_3 which cannot be reduced by crown ethers, or to the formation of unreactive $[FeX_2^+/12C4][FeX_4^-]$
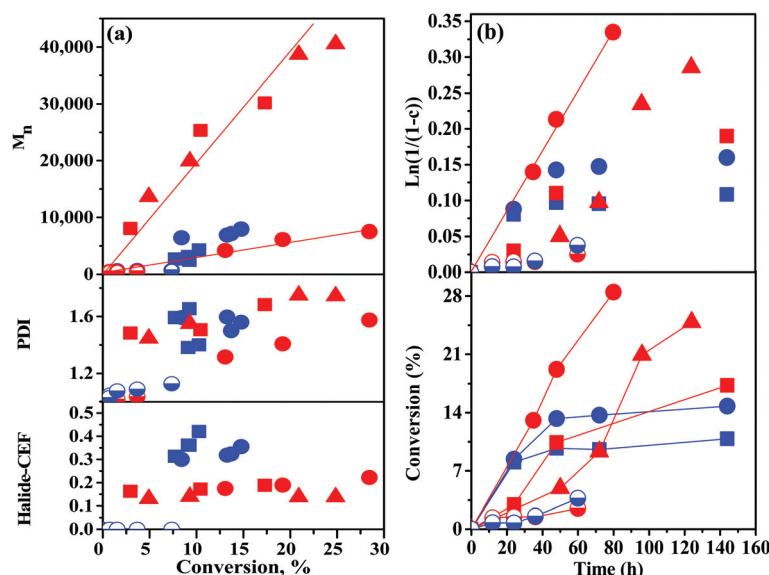

Fig. 6 Iron complexes with crown ether ligands (a) dependence of M_n, PDI and Br-CEF on conversion, (b) kinetics. [BD]/[DB3]/[$FeCl_2$ or $FeBr_2$]/[12C4] = 100/1/2/4, (◑, ◐); [BD]/[DB3]/[TBPO]/[$FeCl_3$ or $FeBr_3$]/[L] = 100/1/0.2/0.05/0.15; 12C4 (●, ●), 15C5 (■, ■), DB18C6 (▲, none).

complexes[65b] analogue to the case of Bu₄NX, or to an irreversible Fe-OMRP contribution.

Phosphines and photo-ATRP

Phosphines have been widely used in the Fe-ATRP of St and MMA,[47] and their lower nucleophilicity *vs.* amines should be beneficial in BD-ATRP. Of interest here is also the use of cata-

lytic procedures with phosphines as reducing agents, especially in conjunction with light irradiation.[51]

The effect of TTMPP is demonstrated first for N-ATRP with FeCl₂, FeCl₃, FeBr₂ and FeBr₃ (Fig. 7) followed by a comparison of ICAR and catalytic regular and photo ATRP (Fig. 8), control ligand-free polymerizations (Fig. 9) and N- and photo ATRP comparisons (Fig. 10).
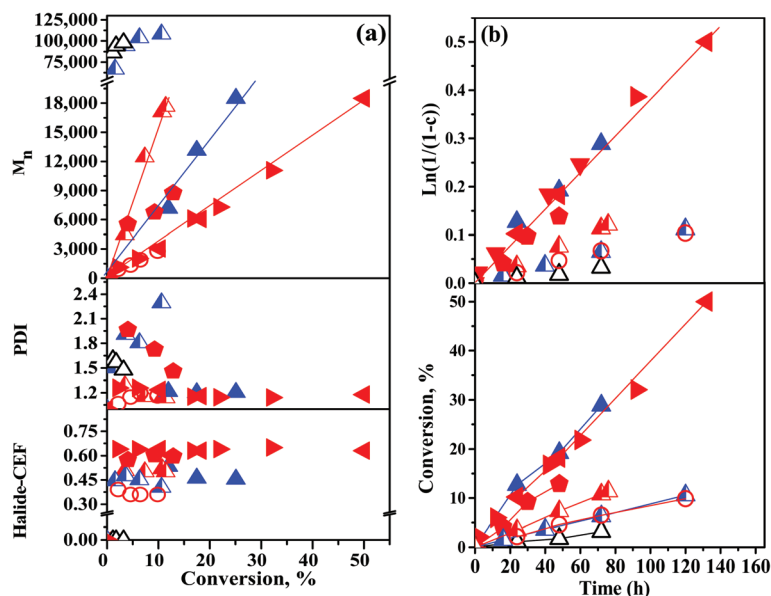

Fig. 7 N-ATRP of BD with phosphine ligands. (a) Dependence of M_n, PDI and Br-CEF on conversion, (b) kinetics. [BD]/[FeCl₃ or FeBr₃]/[L] = 100/1/2 (△), [BD]/[DB3]/[FeCl₂ or FeBr₂]/[TTMPP] = 100/1/2/3, (▲, ▲), [BD]/[DB3]/[FeCl₃ or FeBr₃]/[TTMPP] = 100/1/2/3 (◀, ▶ duplications, ▲), [BD]/[DCPX]/[FeCl₃]/[TTMPP] = 100/1/2/3 (⬟), [BD]/[DB3]/[FeCl₃]/[P(t-Bu)₃] = 100/1/2/3 (◯).
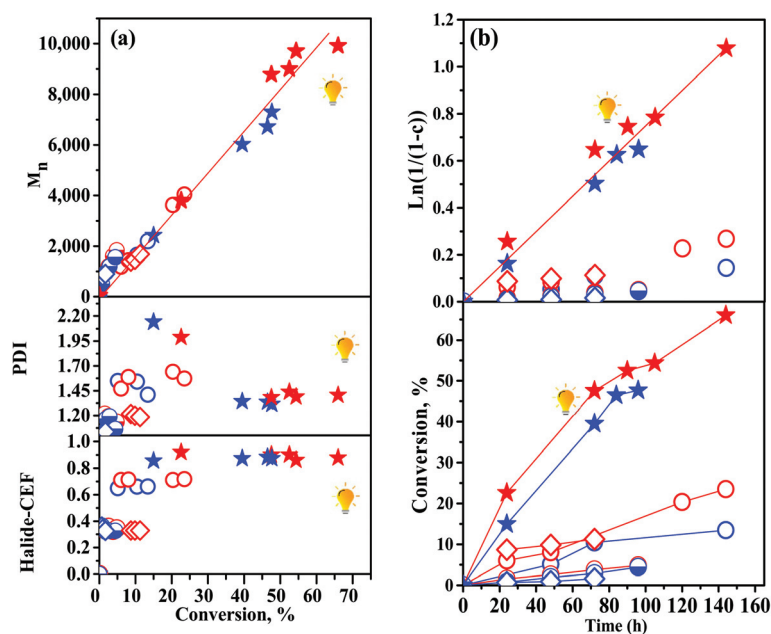

Fig. 8 Light *vs.* TBPO *vs.* TTMPP or PPh₃ as reducing agents in the FeX₃ mediated BD-ATRP at catalytic Fe levels. (a) Dependence of M_n, PDI and Br-CEF on conversion, (b) kinetics. [BD]/[DB3]/[TBPO]/[FeCl₃ or FeBr₃]/[TTMPP] = 100/1/0/0.05/0.15; dark: (◯, ●), BLB: (★, ★), and **ICAR** 100/1/0.2/0.05/0.15, L = TTMPP (◯, ◯) and PPh₃ (◇, ◇).
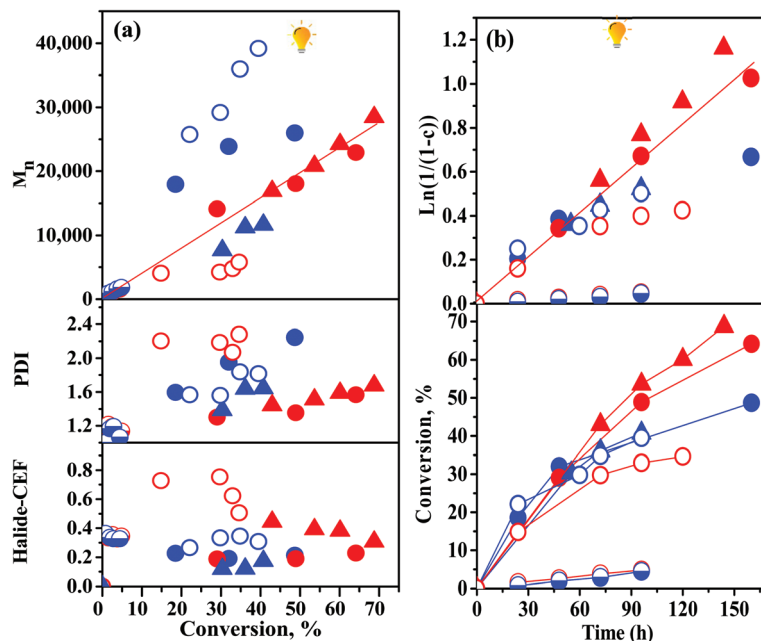
Fig. 9 Ligand-free, photomediated Fe-BD-ATRP with and without R−X initiator. (a) Dependence of M_n, PDI and Br-CEF on conversion, (b) kinetics. [BD]/[DB3]/[FeCl$_3$ or FeBr$_3$] = 100/0/1 (BLB: ●, ●; BLED: ▲, ▲); 100/1/0.05 (BLB: ○, ○); [BD]/[DB3]/[FeCl$_3$ or FeBr$_3$]/[TTMPP] = 100/1/0.05/0.15 dark (◐, ◑).
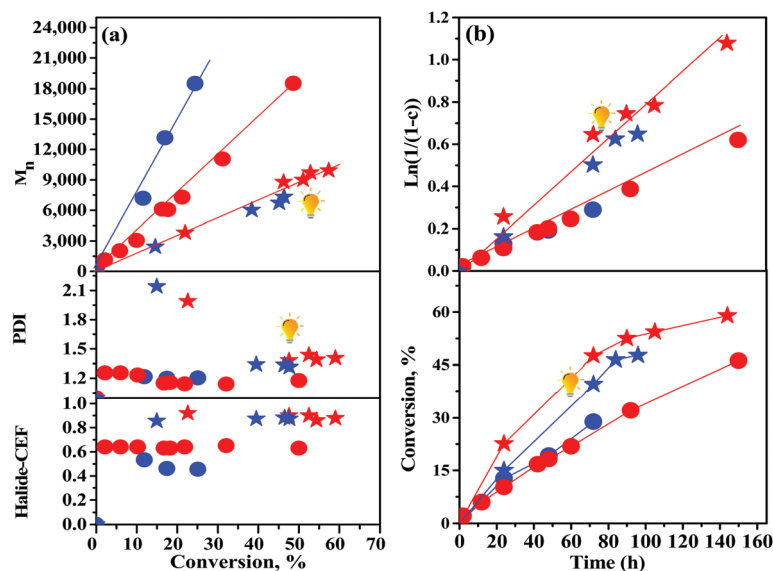

Fig. 10 N- and photo-BD-ATRP with TTMPP with and without irradiation, (a) Dependence of M_n, PDI and Br-CEF on conversion, (b) kinetics. [BD]/[DB3]/[FeCl$_3$ or FeBr$_3$]/[TTMPP] = 100/1/0.05/0.15 BLB (★, ★), 100/1/2/3 (●, ●).

The evaluation of phosphines (PR$_3$, R = n-Bu, t-Bu, C$_6$H$_5$, C$_6$H$_4$-4-CF$_3$, C$_6$F$_5$, and C$_6$H$_2$-2,4,6-(OCH$_3$)$_3$, $i.e.$ TTMPP) in N-ATRP with FeCl$_2$, FeCl$_3$, FeBr$_2$ and FeBr$_3$ (Fig. 7) reconfirms the FeX$_3$ > FeX$_2$ and Cl ≫ Br trend in ATRP quality observed throughout this study. As seen for styrene,[51] consistent with the much lower ligand basicity, no polymerization occurs in N-ATRP with FeX$_3$ for PPh$_3$ as well for phosphines with elec-

tron withdrawing P(C$_6$H$_4$-4-CF$_3$)$_3$, P(C$_6$F$_5$)$_3$ or poorly donating (n-Bu) groups. By contrast, the more basic/reducing P(t-Bu)$_3$[67] affords a linear M_n dependence on conversion for FeCl$_3$/P(t-Bu)$_3$, while TTMPP[51] is efficient in all cases except FeBr$_2$. Here, although both FeCl$_2$ ≫ FeBr$_2$ polymerizations proceed to only ~10% conversion and present very similar linear kinetics (k_p^{app} = 1.6 × 10^{-3} h^{-1} $vs.$ 9 × 10^{-4} h^{-1}) and X-CEFs (0.5 $vs.$ 0.45),

$FeBr_2$ leads to a poor control with high M_n (60–100 000) and PDI (1.6–2.4) values, whereas $FeCl_2$ has much better initiator efficiency and remarkably low PDI ~ (1.3–1.15). The situation improves for FeX_3, but the $FeCl_3 \gg FeBr_3$ persists. Both polymerizations are now much faster ($k_p^{app} = 4.1 \times 10^{-3}$ h^{-1}) and both display linear M_n vs. conversion profiles, but with much higher conversion (50% vs. 25%), better initiator efficiency, lower PDI (1.15 vs. 1.2) and higher X-CEF (0.65 vs. 0.45) for $FeCl_3$. Moreover, CRP features are obtained even with a relatively poor initiator such a primary benzyl chloride (DCPX), and $FeCl_3$. The better results, especially the lower PDI, afforded by $FeX_3 > FeX_2$ stem from the immediate availability of the deactivator from the polymerization onset (i.e. not derived from early termination).

Decreasing the FeX_3 concentration in N-ATRP to catalytic ICAR-like ratios (Fig. 8), leads to much slower reactions ($k_p^{app} = 4 \times 10^{-4}$ h^{-1}) and lower conversions (~5%) and X-CEFs ~ 0.35 for both, indicating that at low levels, TTMPP alone is not sufficient for a good polymerization, and that in catalytic systems, TBPO or light are still needed to prevent FeX_3 accumulation.

Accordingly, TBPO promoted ICARs (Fig. 8) reinforce the $FeCl_3 > FeBr_3$ trend for PPh_3 and especially for TTMPP and are both faster CRPs than the corresponding catalytic N-ATRPs ($k_p^{app} = 1.9 \times 10^{-3}$ h^{-1} vs. 1.4×10^{-3} h^{-1}), proceed to higher conversion (~13% and ~25%), and with a similar M_n slope, but with higher PDI (~1.5–1.6) and higher Br-CEF (0.65–0.7). Yet, they remain inferior to regular N-ATRP in terms of conversion, rate and especially PDI. Indeed, for $FeCl_3 > FeBr_3$, both procedures afford control, but the IE and X-CEF (0.7 vs. 0.6) is higher for ICAR and the PDI is lower (1.15 vs. 1.6) whereas the rate is twice as fast in N-ATRP (4.1×10^{-3} vs. 1.9×10^{-3}).

However, the situation is reversed upon photoirradiation of a catalytic N-ATRP (Fig. 8). Here, for both FeX_3 systems, and similarly to Bu_4NCl examples above, upon BLB (black light bulb) irradiation, photo-ATRP provides much higher conversion (50% and ~70%), with the fastest rates in this set (7 and 9×10^{-3} h^{-1}), which are about two, five and respectively twenty times those of N-ATRP, ICAR and dark catalytic N-ATRP. The initiator efficiency remains the same as in ICAR, and while the PDI values are initially high, they quickly drop to ~1.3 and 1.4 for $FeBr_3$ and respectively $FeCl_3$. Most importantly, the X-CEF is very high in both cases, and hovers between 0.85 and 0.9.

To further clarify the effect of the reaction variables, a set of control polymerizations were carried out under irradiation without a ligand and with or without an R–X initiator (Fig. 9). As seen above, TTMPP alone barely affords trace polymerization. Similarly, no polymer is obtained in the dark from BD/$FeCl_3$. Interestingly, polymer is obtained in a CRP manner in photo-ATRP under both BLB and blue LED (BLED) irradiation even in the absence of an R–X alkyl halide or TBPO initiator and of a ligand, using only BD/FeX_3 = 100/1. Thus, ligand-free FeX_3 is capable of both BD initiation via photolysis to FeX_2 and X$^\bullet$, as well as of reversible deactivation of the propagating PBD$^\bullet$ radicals even in a non-polar toluene/BD media.

Indeed, for BLB, both $FeCl_3$ and $FeBr_3$ display an initial similar rate (k_p^{app} ~ 6.6×10^{-3} h^{-1} which levels off for $FeBr_3$), X-CEFs of ~0.2 and parallel M_n profiles which increase linearly with conversion. Again, $FeCl_3$ produces higher conversion (65 vs. 50%) and a better CRP with a lower M_n intercept (~origin vs. ~14 000) and narrower PDI (1.3–1.6) vs. (1.6–2.3) than $FeBr_3$.

Under BLED irradiation, the polymerization control improves especially for $FeBr_3$, where the conversions and rates increase somewhat vs. BLB, and $FeCl_3$ remains faster than $FeBr_3$ (k_p^{app} ~ 8×10^{-3} h^{-1} vs. k_p^{app} ~ 6×10^{-3} h^{-1}), proceeds to much higher conversion (~70 vs. 40%) and affords higher X-CEF (~0.4 vs. ~0.15). Both catalysts present similar M_n profiles with a very low M_n intercept, and the PDI decreases vs. BLB for $FeBr_3$ to ~1.4–1.65 and increases only slightly to 1.45–1.7 for $FeCl_3$ and again increases with conversion from ~1.4 to ~1.7 for both. In addition, while the Br-CEF is lower under BLED, Cl-CEF is higher than for BLB (~0.4 vs. 0.2), but does decrease with conversion (0.45–0.3). While BLB is higher energy, the glass tube does filter out the UV component, which may explain while better results are obtained with blue LED.

Conversely, a comparison of the ligand-free catalytic photo-ATRP with [BD]/[DB3]/[FeX_3] = 100/1/0.05 with the corresponding catalytic [BD]/[DB3]/[FeX_3]/[TTMPP] = 100/1/0.05/0.15 in the dark reveals the clear superiority of light vs. catalytic TTMPP as a reducing agent.

In all four BD/FeX_3 photo-ATRP cases here, the PDIs increase with conversion and are higher, while the X-CEFs are lower than in N-ATRP. This is a consequence of the continuously decreasing FeX_3 deactivator concentration via X$^\bullet$ initiation and corresponding continuous increase in the concentration of the FeX_2 activator. The reaction is equivalent with the 1,4-radical dihalogenation of BD, which through polymerization produces a difunctional X-PBD-X by FeX_3 termination of the growing chain. Due to the continuous initiation of new chains, irradiation thus substantially improves (doubles) the rates and conversions (30–60%) by comparison with dark N-ATRP reactions. In addition, difunctional initiators afford better results in CRPs due to the minimization of the effects of termination.[28]

Furthermore, a comparison of all FeX_3/BLB experiments with and without TTMPP and with and without DB3 indicates that while rates are not significantly affected, better control, PDI and X-CEF are obtained for Cl > Br and for BD/DB3/FeX_3/TTMPP = 100/1/0.05/0.15 > BD/FeX_3 = 100/1 and BD/DB3/FeX_3 = 100/1/0.05. However, BD/DB3/FeX_3 affords higher X-CEF while BD/FeX_3 provides lower PDI likely due to the higher FeX_3 concentration.

Fig. 10 highlights the most successful polymerizations from this series, i.e. the N-ATRP with [BD]/[DB3]/[FeX_3]/[TTMPP] = 100/1/2/3 and the corresponding catalytic photo-ATRP with 100/1/0.05/0.15 under BLB. Here, again $FeCl_3 \gg FeBr_3$ and higher conversions (65% vs. 45%) with faster rates (8 vs. 4 $\times 10^{-3}$ h^{-1}), better X-CEFs (0.9 vs. 0.65) and initiator efficiency are afforded by photo-ATRP, while N-ATRP is superior in PDI (1.15–1.2 vs. 1.3–1.4).

Halide chain ends trends

Fig. 11 illustrates the dependence of all possible types of PBD-X chain ends (*i.e.* 1,2- and 1,4-*cis* and *trans* Cl and Br) during a stoichiometric N-ATRP ([BD]/[DB3]/[FeCl₃]/[TTMPP] = 100/1/2/3) which proceeds with a Br initiator (DB3) and a Cl based catalyst (FeCl₃), where the overall Br/Cl mole ratio is 1/3. Unlike simple St or acrylate monomers which afford only two types of halide chain ends in mixed halide ATRP systems, PBD will afford 6. Several interesting macromolecular halogen exchange[68] effects which support the superiority of FeCl₃ *vs.* FeBr₃ are observed.

Remarkably, the total (Cl + Br) X-CEF values remain constant at ~65% with increasing conversion, indicating that various side reactions do not progress during polymerization and are minimized.

Here, the expected 1,4-*trans* > 1,4-*cis* > 1,2-trend in relative ratios in maintained not only in the PBD microstructure, but also in the initiator addition to BD, as well as in allyl chain halide stability and reactivity. More interestingly, within each set, the total (Cl + Br)-CEF is also almost constant, where a slight decrease for the total 1,4-*cis* X-CEF is compensated by a slight increase for the 1,2-X-CEF. However, due to the stronger allyl–Cl *vs.* allyl–Br bond,[32] and consistent with the mixed halide Cu-ATRP of other monomers,[67] the Cl-CEF increases and the Br-CEF decreases with conversion in each category in an almost linear fashion and indicates that complete Br to Cl exchange should occur at higher conversion.
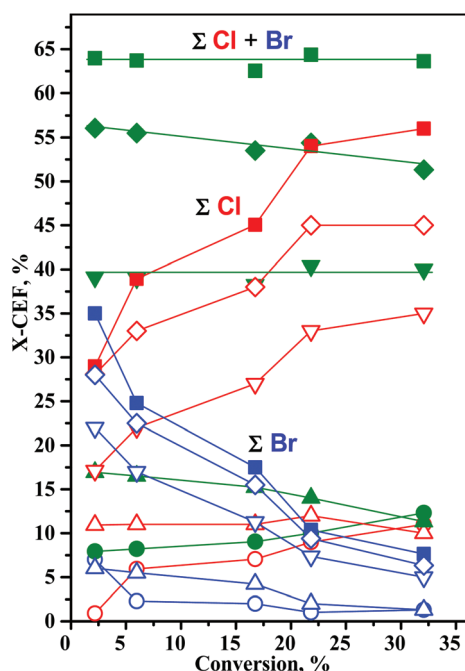
A similar trend to the Cl-CEF above was seen for the Br-CEFs in BD-ATRP with bromine-only systems (*e.g.* ICAR, BD/R–Br/TBPO with either CuBr₂ or (PPh₃)Ni(CO)₂),[30] where in line with the higher stability of *trans* *vs.* *cis* chain ends, the total Br-CEF remained constant, but the 1,4-*trans* Br-CEF increased and the 1,4-*cis* Br-CEF decreased with conversion. Since the total X-CEF profiles are flat in these mixed halide systems, it is likely that the rate of 1,4-*trans* Br-CEF accumulation is closely matched by the rate of Br to Cl halogen exchange. Thus, while the more stable 1,4-*trans* chain ends should accumulate to the detriment of the less stable 1,4-*cis* chain ends for both halides, the concomitant Br to Cl halide exchange exactly balances this effect and leads to flat X-CEF profiles. The overall patterns in the accumulation of the more stable chain end are similar with the trends from the IDT of VDF.[28]

While comparing Fe and Cu homo- and mixed halide systems, it appears that for a better BD-ATRP, Fe favors Cl where Cu favors Br chain ends. Since PBD-Cl are more stable and less susceptible to side reactions than PBD-Br, this implies that the FeCl₂/FeCl₃ (alone or with TTMPP) is a better activator/deactivator than FeBr₂/FeBr₃ and CuBr/CuBr₂/bpy for PBD-X/PBD•.

On the other hand, the high X-CEF values especially in the stoichiometric N-ATRP above are also somewhat surprising, especially in view of how basic TTMPP is (pK_a = 11.2),[69] and that it easily quaternizes[68] even deactivated alkyl halides, albeit in the more polar EtOH. It is thus likely that by contrast with amine ligands, the kinetics of the TTMPP reduction of FeX₃ are faster than those of chain end quaternization. This could result from the decrease in the TTMPP nucleophilicity due to the steric effect of its very large cone angle (188° *vs.* 145° for PPh₃),[70] and the steric crowding associated with the PBD-X polymer chain end. As such, the excess Lewis basic TTMPP remaining after the formation of a very strong complex with the highly Lewis acidic FeX₃ in N-ATRP only serves as a reducing agent to form [TTMPPBr]⁺Br⁻ [51] and apparently does not react with the chain ends especially in the nonpolar toluene, which minimizes PBD-X reactions with nucleophiles.

Conversely, the higher stability of PBD-Cl *vs.* PBD-Br, in addition to the different halophilicity[4–7] of FeX$_n$Y$_m$ (X, Y = Cl, Br, $m + n$ = 2 or 3) explains the superiority of FeCl$_x$ over FeBr$_x$ across all systems investigated herein. However, while CuBr₂ is known to be a better deactivator than CuCl₂,[67] the k_{deact} values of FeCl₃ *vs.* FeBr₃ have not been quantitatively addressed in the ATRP literature.

Fig. 11 Dependence of the PBD-X (X = Cl, Br) and total = Cl + Br chain end functionality (CEF) on conversion in N-ATRP with [BD]/[DB3]/[FeCl₃]/[TTMPP] = 100/1/2/3. CEF: 1,2 (○, ◯, ●); 1,4-*cis* (△, △, ▲); 1,4-*trans* (▽, ▽, ▼); 1,4-*cis* + *trans* (◇, ◇, ◆); (1,2 + 1,4-*cis* + 1,4-*trans*) (□, □, ■).

Conclusions

Owing to a low b_p, very low k_p, Diels–Alder cycloaddition and to the poor stability of the labile allyl halide termini, the ATRP of dienes remains a significant polymer chemistry challenge. In this study, the ligand (L) and halide effects of a series of iron complexes (FeX₂ or FeX₃, X = Cl, Br)/L supported by carbon (Cp₂Fe₂(I)(CO)₄ > Cp₂Fe > Fe(CO)₅ > (Ph₂PCp)₂Fe), nitrogen (phthalocyanine ≫ bpy ≥ MeO-bpy ≫ PMDETA >

phen), halide (FeX$_m$Y$_{4-m}$/Bu$_4$N, X, Y = Cl ≫ Br > I), oxygen (12-crown-4 ≫ 15-crown-5 ≥ dibenzo-18-crown-6) and phosphorous (P[Ph(2,4,6-OMe)$_3$]$_3$ > P(t-Bu)$_3$ ≫ P(n-Bu)$_3$, PPh$_3$, P[Ph(4-CF$_3$)]$_3$, P(C$_6$F$_5$)$_3$) ligands, as well as ligand-free FeX$_3$, were evaluated in the normal, ICAR, and photo-ATRP of butadiene initiated from bromoesters, α,α-dichloro-p-xylene, or FeX$_3$ in toluene at 110 °C.

While a quantitative comparison across all ligands and procedures is incomplete as not all possible FeX$_{2,3}$/L/(ATRP procedure) combinations are available, in addition to the qualitative ligand order seen above in each class, the following TTMPP (0.3–0.7) > Bu$_4$NX (0.1–0.7) > crown ethers (0.15–0.35) > amines (0–0.18, except FePC ~ 0.45) and C-ligands (0–0.1, except (Ph$_2$PCp)$_2$Fe ~ 0.8) trend was seen in terms of X-CEF, and clear FeCl$_2$ ≫ FeBr$_2$ and respectively, FeCl$_3$ ≫ FeBr$_3$ trends were observed in terms of overall control. These overriding Cl ≫ Br and TTMPP ≫ all L effects occur consistently across all ligands, ATRP protocols or reaction conditions in terms of CRP quality (better initiator efficiency, lower PDI, faster kinetics, higher conversion and X-CEF).

The Cl ≫ Br effect correlates with the higher stability of the allyl PBD-Cl vs. PBD-Br chain ends to side reactions such as thermal dehalogenation or ligand quaternization as demonstrated by the PBD-Cl preferential accumulation in mixed halide systems, and with FeCl$_3$ likely being a better deactivator than FeBr$_3$ towards allyl radicals. Conversely, while basic enough to reduce FeX$_3$, TTMPP is apparently not nucleophilic enough to quaternize PBD-X, especially in nonpolar toluene and successfully enables a faster activation/deactivation equilibrium than all other ligands.

As such, even in unoptimized experiments, Fe/TTMPP consistently outperforms all other ligands or complexes regardless of the ATRP procedure in terms of PDI, rate and X-CEF and enables e.g. N-ATRP with BD/DB3/FeCl$_3$/TTMPP = 100/1/2/3 to afford a clean CRP profile with PDI as low as 1.15–1.2 and CEF = 0.65 at up to 50% conversion. Furthermore, while CRP features are obtained in photo-ATRP even in the absence of ligand and initiator, BLB or BLED irradiation of a catalytic N-ATRP with BD/DB3/FeCl$_3$/TTMPP = 100/1/0.05/0.15 significantly improve the polymerization rate (×10 vs. dark reactions), conversion (up to 70%) and X-CEF (0.9) via the additional initiation afforded by FeX$_3$ photolysis, albeit with a slight increase in PDI to ~1.4. While it is not clear at this point what the ligand effect is on the rate of photolysis of Fe complexes, it is expected that irradiation would significantly improve all other Fe/L polymerizations, as seem for e.g. Bu$_4$NCl.

Thus, Fe-mediated BD-ATRP is achievable, and the rational selection of the polymerization variables enables minimization of side reactions and the successful synthesis of well-defined PBD with a wide range of molecular weights and narrow PDI, reasonably high X-CEF, suitable for the preparation of e.g. block copolymers.

As the conditions for successful BD-ATRP are beginning to emerge for various transition metal or organic catalysts, they can guide the optimization of the ATRP of other dienes and the elaboration of their industrially significant emulsion (co)polymerizations. Indeed, whereas these solution polymerizations were performed in glass tubes at about a few atm., which hardly affect rate constants,[71] better quality diene-ATRPs are expected[24,70] in high pressure emulsion polymerizations due to both the large increase in k_p/k_t,[72] and the faster kinetics of emulsion polymerization. Research along these lines is in progress and will be reported soon.

Conflicts of interest

There are no conflicts to declare.

Acknowledgements

References

1 G. Odian, *Principles of Polymerization*, Wiley, New York, 4th edn, 2004, ch. 3, p. 311.

2 M. Schöps, H. Leist, A. DuChesne and U. Wiesner, *Macromolecules*, 1999, **32**, 2806–2809.

3 (a) A. Hirao and M. Hayashi, *Acta Polym.*, 1999, **50**, 219–231; (b) W. J. Evans, D. G. Giarikos and N. T. Allen, *Macromolecules*, 2003, **36**, 4256–4257.

4 (a) W. A. Braunecker and K. Matyjaszewski, *J. Mol. Catal. A: Chem.*, 2006, **254**, 155–164; (b) W. A. Braunecker and K. Matyjaszewski, *Prog. Polym. Sci.*, 2007, **32**, 93–146; (c) T. Pintauer, K. Matyjaszewski and Z. Guan, *Top. Organomet. Chem.*, 2009, **26**, 221–251; (d) N. V. Tsarevsky and K. Matyjaszewski, *RSC Polym. Chem. Ser.*, 2013, vol. 4, ch. 8, pp. 287–357.

5 (a) F. di Lena and K. Matyjaszewski, *Prog. Polym. Sci.*, 2010, **35**, 959–1021; (b) M. Ouchi, T. Terashima and M. Sawamoto, *Chem. Rev.*, 2009, **109**, 4963–5050; (c) L. Fetzer, V. Toniazzo, D. Ruch and F. di Lena, *Isr. J. Chem.*, 2012, **52**, 221–229.

6 K. Matyjaszewski and J. Spanswick, in *Polymer Science: A Comprehensive Reference*, ed. K. Matyjaszewski and M. Möller, Elsevier, Amsterdam, 2012, vol. 3, pp. 377–428.

7 K. Matyjaszewski, *Macromolecules*, 2012, **45**, 4015–4039.

8 G. Huybrechts, L. Luyckx, T. Vandenboom and B. Van Mele, *Int. J. Chem. Kinet.*, 1977, **9**, 283–293.

9 (a) M. Kamachi and A. Kajiwara, *Macromolecules*, 1996, **29**, 2378–2382; (b) S. Beuermann and M. Buback, *Prog. Polym. Sci.*, 2002, **27**, 191–254.

10 P. A. Weerts, A. L. German and R. G. Gilbert, *Macromolecules*, 1991, **24**, 1622–1628.

11 (a) D. Benoit, E. Harth, P. Fox, R. M. Waymouth and C. J. Hawker, *Macromolecules*, 2000, **33**, 363–370; (b) S. Harrisson, P. Couvreur and J. Nicolas, *Macromolecules*, 2011, **44**, 9230–9238.

12 (a) D. S. Germack and K. L. Wooley, *J. Polym. Sci., Part A: Polym. Chem.*, 2007, **45**, 4100–4108; (b) G. Moad, *Polym. Int.*, 2017, **66**, 26–41.

13 Y. Nakamura, T. Arima, S. Tomita and S. Yamago, *J. Am. Chem. Soc.*, 2012, **134**, 5536–5539.

14 P. Lebreton, B. Ameduri, B. Boutevin, J. Corpart and D. Juhue, *Macromol. Chem. Phys.*, 2000, **201**, 1016–1024.

15 A. Debuigne, C. Jerome and C. Detrembleur, *Angew. Chem., Int. Ed.*, 2009, **48**, 1422–1424.

16 (a) A. D. Asandei, H. S. Yu and C. P. Simpson, *Polym. Mater.: Sci. Eng.*, 2010, **103**, 511–512; (b) A. D. Asandei, H. S. Yu and C. P. Simpson, *Polym. Mater.: Sci. Eng.*, 2010, **102**, 68–69; (c) A. D. Asandei and H. S. Yu, *Polym. Prepr.*, 2009, **50**(2), 601–602; (d) A. D. Asandei, H. S. Yu and O. Adebolu, *Polym. Mater.: Sci. Eng.*, 2009, **101**, 1377–1378; (e) A. D. Asandei, H. S. Yu and C. P. Simpson, *Polym. Mater.: Sci. Eng.*, 2009, **101**, 1379–1380.

17 (a) A. D. Asandei, C. P. Simpson, H. S. Yu, O. Adebolu, G. Saha and Y. Chen, *ACS Symp. Ser.*, 2009, **1024**, 149–166; (b) A. D. Asandei and C. P. Simpson, *Polym. Prepr.*, 2008, **49**(2), 75–76; (c) A. D. Asandei, H. S. Yu and C. P. Simpson, *Polym. Prepr.*, 2010, **51**(2), 584–585; (d) A. D. Asandei, H. S. Yu and C. P. Simpson, *Polym. Prepr.*, 2010, **51**(1), 545–546; (e) A. D. Asandei, O. Adebolu, H. S. Yu, C. P. Simpson and M. Gilbert, *Polym. Prepr.*, 2009, **50**(1), 177–178; (f) A. D. Asandei, H. S. Yu, O. Adebolu, C. P. Simpson and O. Duong, *Polym. Mater.: Sci. Eng.*, 2009, **100**, 366–367; (g) A. D. Asandei and C. Simpson, *Polym. Prepr.*, 2008, **49**(1), 452–453; (h) A. D. Asandei, C. P. Simpson and H. S. Yu, *Polym. Prepr.*, 2008, **49**(2), 73–74; (i) A. D. Asandei and C. Simpson, *Polym. Prepr.*, 2008, **49**(1), 452–453; (j) A. D. Asandei and G. Saha, *Polym. Prepr.*, 2005, **46**(2), 474–475.

18 (a) A. D. Asandei, C. P. Simpson, A. Olumide and H. S. Yu, *Polym. Prepr.*, 2010, **51**(1), 553–554; (b) A. D. Asandei, H. S. Yu and C. P. Simpson, *Polym. Prepr.*, 2010, **51**(2), 586–587; (c) A. D. Asandei, C. P. Simpson, A. Olumide and H. S. Yu, *Polym. Mater.: Sci. Eng.*, 2010, **102**, 425–426; (d) A. D. Asandei, C. P. Simpson, A. Olumide and H. S. Yu, *Polym. Prepr.*, 2010, **51**(1), 498–499; (e) A. D. Asandei, H. S. Yu, O. Adebolu and C. P. Simpson, *Polym. Prepr.*, 2011, **52**(2), 470–471; (f) A. D. Asandei and G. Saha, *Polym. Prepr.*, 2005, **46**(1), 674–675.

19 (a) R. Poli, *Chem. – Eur. J.*, 2015, **21**, 6988–7001; (b) R. Poli, *Eur. J. Inorg. Chem.*, 2011, **10**, 1513–1530; (c) R. Poli, *Angew. Chem., Int. Ed.*, 2006, **45**, 5058–5070.

20 (a) A. D. Asandei and I. W. Moran, *J. Am. Chem. Soc.*, 2004, **126**, 15932–15933; (b) A. D. Asandei and G. Saha, *Macromol. Rapid Commun.*, 2005, **26**, 626–631.

21 (a) A. D. Asandei, Y. Chen, G. Saha and I. W. Moran, *Tetrahedron*, 2008, **64**, 11831–11838; (b) A. D. Asandei, Y. Chen, O. I. Adebolu and C. P. Simpson, *J. Polym. Sci., Part A: Polym. Chem.*, 2008, **46**, 2869–2877; (c) A. D. Asandei, Y. Chen, I. W. Moran and G. Saha, *J. Organomet. Chem.*, 2007, **692**, 3174–3182;

(d) A. D. Asandei and Y. Chen, *Macromolecules*, 2006, **39**, 7459–7554.

22 (a) A. D. Asandei, Y. Chen, C. Simpson, M. Gilbert and I. W. Moran, *Polym. Prepr.*, 2008, **49**(1), 489–490; (b) A. D. Asandei, Y. Chen and O. Adebolu, *Polym. Mater.: Sci. Eng.*, 2008, **98**, 370–371; (c) A. D. Asandei and G. Saha, *Polym. Prepr.*, 2007, **48**(2), 272–273; (d) A. D. Asandei and Y. Chen, *Polym. Mater.: Sci. Eng.*, 2007, **97**, 450–451.

23 (a) A. D. Asandei, C. P. Simpson, H. S. Yu, O. I. Adebolu, G. Saha and Y. Chen, *ACS Symp. Ser.*, 2009, **1024**, 149–166; (b) A. D. Asandei and C. P. Simpson, *Polym. Prepr.*, 2008, **49**(2), 75–76; (c) A. D. Asandei, C. P. Simpson and H. S. Yu, *Polym. Prepr.*, 2008, **49**(2), 73–74; (d) A. D. Asandei and G. Saha, *Polym. Prepr.*, 2005, **46**(2), 474–475.

24 M. Zhong and K. Matyjaszewski, *Macromolecules*, 2011, **44**, 2668–2677.

25 (a) J. Wang and K. Matyjaszewski, *Macromolecules*, 1995, **28**, 7901–7910; (b) V. Percec and B. Barboiu, *Macromolecules*, 1995, **28**, 7970–7972; (c) M. Kato, M. Kamigaito, M. Sawamoto and T. Higashimura, *Macromolecules*, 1995, **28**, 1721–1723.

26 V. Percec, T. Guliashvili, J. S. Ladislaw, A. Wistrand, A. Stjerndahl, M. J. Sienkowska, M. J. Monteiro and S. Sahoo, *J. Am. Chem. Soc.*, 2006, **128**, 14156–14165.

27 J. Xia, H. Paik and K. Matyjaszewski, *Macromolecules*, 1999, **32**, 8310–8314.

28 (a) A. D. Asandei, O. I. Adebolu and C. P. Simpson, *J. Am. Chem. Soc.*, 2012, **134**, 6080–6083; (b) A. D. Asandei, O. I. Adebolu, C. P. Simpson and J. Kim, *Angew. Chem., Int. Ed.*, 2013, **52**, 10027–10030; (c) A. D. Asandei, O. I. Adebolu and C. P. Simpson, *ACS Symp. Ser.*, 2012, **1106**, 47–63; (d) A. D. Asandei, O. I. Adebolu and C. P. Simpson, *Handbook of Fluoropolymer Science and Technology*, John Wiley & Sons, Inc., 2014, ch. 2, pp. 21–42; (e) C. P. Simpson, O. I. Adebolu, J. S. Kim, V. Vasu and A. D. Asandei, *ACS Symp. Ser.*, 2015, **1187**, 183–209; (f) P. Cernoch, S. Petrova, Z. Cernochova, J. S. Kim, C. P. Simpson and A. D. Asandei, *Eur. Polym. J.*, 2015, **68**, 460–470; (g) F. C. Sun, A. M. Dongare, A. D. Asandei, S. P. Alpay and S. Nakhmanson, *J. Mater. Chem. C*, 2015, **3**, 8389–8396; (h) C. P. Simpson, O. I. Adebolu, J. S. Kim, V. Vasu and A. D. Asandei, *Macromolecules*, 2015, **48**, 6404–6420; (i) A. D. Asandei, *Chem. Rev.*, 2016, **116**, 2244–2274; (j) A. Ghosh, L. Louis, A. D. Asandei and S. Nakhmanson, *Soft Mater.*, 2018, **14**, 2484–2491.

29 (a) J. Wootthikanokkhan, M. Peesan and P. Phinyocheep, *Eur. Polym. J.*, 2001, **37**, 2063–2071; (b) S. U. Heo, G. H. Rhee, D. H. Lee, J. H. Kim, D. S. Choi and D. W. Lee, *J. Ind. Eng. Chem.*, 2006, **12**, 241–247; (c) J. Hua, H. Xu, J. Geng, Z. Deng, L. Xu and Y. Yu, *J. Polym. Res.*, 2011, **18**, 41–48; (d) J. Li, J. El-harfi, S. M. Howdle, K. Carmichael and J. D. Irvine, *Polym. Chem.*, 2012, **3**, 1495–1501.

30 (a) H. S. Yu, J. S. Kim, V. Vasu, C. P. Simpson and A. D. Asandei, 2018, submitted; (b) A. D. Asandei, *US Pat,*

9862689B2, 2018; (c) V. Vasu, J. S. Kim, H. S. Yu, W. I. Bannerman, M. E. Johnson and A. D. Asandei, *ACS Symp. Ser.*, 2018, in press.

31 (a) A. D. Asandei and S. H. Yu, *Polym. Prepr.*, 2011, **52**(2), 584–585; (b) A. D. Asandei and S. H. Yu, *Polym. Prepr.*, 2011, **52**(2), 564–565; (c) A. D. Asandei, C. P. Simpson, O. Adebolu and Y. Chen, *Polym. Prepr.*, 2011, **52**(2), 759–560; (d) A. D. Asandei and H. S. Yu, *Polym. Prepr.*, 2011, **52**(1), 415–416; (e) A. D. Asandei and H. S. Yu, *Polym. Prepr.*, 2011, **52**(1), 413–414; (f) A. D. Asandei and H. S. Yu, *Polym. Mater.: Sci. Eng.*, 2011, **104**, 619–620; (g) A. D. Asandei and H. S. Yu, *Polym. Mater.: Sci. Eng.*, 2011, **104**, 627–628.

32 M. B. Gillies, K. Matyjaszewski, P. Norrby, T. Pintauer, R. Poli and P. Richard, *Macromolecules*, 2003, **36**, 8551–8559.

33 K. Matyjaszewski, S. M. Jo, H. Paik and D. A. Shipp, *Macromolecules*, 1999, **32**, 6431–6438.

34 X. Wang, H. Zhao, Y. Li, R. Xiong and X. You, *Top. Catal.*, 2005, **35**, 43–61.

35 W. A. Braunecker, N. V. Tsarevsky, T. Pintauer, R. R. Gil and K. Matyjaszewski, *Macromolecules*, 2005, **38**, 4081–4088.

36 M. Hakansson, K. Brantin and S. Jagner, *J. Organomet. Chem.*, 2000, **602**, 5–14.

37 C. Y. Lin, S. R. A. Marque, K. Matyjaszewski and M. L. Coote, *Macromolecules*, 2011, **44**, 7568–7583.

38 F. Seeliger and K. Matyjaszewski, *Macromolecules*, 2009, **42**, 6050–6055.

39 P. De Paoli, A. A. Isse, N. Bortolamei and A. Gennaro, *Chem. Commun.*, 2011, **47**, 3580–3582.

40 W. Jakubowski, N. V. Tsarevsky, T. Higashihara, R. Faust and K. Matyjaszewski, *Macromolecules*, 2008, **41**, 2318–2323.

41 S. Deibert and F. Bandermann, *Makromol. Chem.*, 1993, **194**, 3287–3299.

42 J. Lutz and K. Matyjaszewski, *J. Polym. Sci., Part A: Polym. Chem.*, 2005, **43**, 897–910.

43 N. V. Tsarevsky, W. A. Braunecker and K. Matyjaszewski, *J. Organomet. Chem.*, 2007, **692**, 3212–3222.

44 Y. Wang, N. Soerensen, M. Zhong, H. Schroeder, M. Buback and K. Matyjaszewski, *Macromolecules*, 2013, **46**, 683–691.

45 A. Anastasaki, C. Waldron, P. Wilson, R. McHale and D. M. Haddleton, *Polym. Chem.*, 2013, **4**, 2672–2675.

46 E. C. F. Ko and K. T. Leffek, *Can. J. Chem.*, 1972, **50**, 1297–1302.

47 Z. Xue, D. Heb and X. Xie, *Polym. Chem.*, 2015, **6**, 1660–1687.

48 R. H. Crabtree, *The organometallic Chemistry of Transition Metals*, Wiley, 6th edn, 2014.

49 A. D. Asandei and V. Percec, *J. Polym. Sci., Part A: Polym. Chem.*, 2001, **39**, 3392–3418.

50 (a) S. Dadashi-Silab, X. Pan and K. Matyjaszewski, *Macromolecules*, 2017, **50**, 7967–7977; (b) C. Chao Bian, Y. N. Zhou, J. K. Guo and Z. H. Luo, *Polym. Chem.*, 2017, **8**, 7360–7368; (c) X. Pan, N. Malhotra, S. Dadashi-Silab and K. Matyjaszewski, *Macromol. Rapid Commun.*, 2017, **38**, 1600651; (d) X. Pan, N. Malhotra, J. Zhang and K. Matyjaszewski, *Macromolecules*, 2015, **48**, 6948–6954.

51 (a) Y. Wang, Y. Kwak and K. Matyjaszewski, *Macromolecules*, 2012, **45**, 5911–5915; (b) H. Schroeder, K. Matyjaszewski and M. Bubac, *Macromolecules*, 2015, **45**, 4431–4437; (c) Y. N. Zhou, J. K. Guo, J. J. Li and Z. H. Luo, *Ind. Eng. Chem. Res.*, 2016, **55**, 10235–10242.

52 (a) H. Schroeder, D. Yalalov, M. Buback and K. Matyjaszewski, *Macromol. Chem. Phys.*, 2012, **213**, 2019–2026; (b) H. Schroeder, M. Buback and K. Matyjaszewski, *Macromol. Chem. Phys.*, 2014, **215**, 44–53; (c) H. Schroeder, M. Buback and M. P. Shaver, *Macromolecules*, 2015, **48**, 6114–6120.

53 H. Schroeder, J. Buback, S. Demeshko, K. Matyjaszewski, F. Meyer and M. Buback, *Macromolecules*, 2015, **48**, 1981–1990.

54 (a) H. Schroeder, K. Matyjaszewski and M. Buback, *Macromolecules*, 2015, **48**, 4431–4437; (b) J. K. Guo, Y. N. Zhou and Z. H. Luo, *Macromolecules*, 2016, **49**, 4038–4046.

55 S. Smolne, M. Buback, S. Demeshko, K. Matyjaszewski, F. Meyer, H. Schroeder and A. Simakova, *Macromolecules*, 2016, **49**, 8088–8097.

56 (a) O. Reihlen, A. Gruhl, G. Hessling and O. Pfrengle, *Liebigs Ann. Chem.*, 1930, **482**, 161; (b) O. Mills and S. G. Robinson, *Acta Crystallogr.*, 1963, **16**, 758; (c) H. Li, H. Feng, W. Sun, Q. Fan, Y. Xie, R. B. King and H. F. Schaefer, *Organometallics*, 2013, **32**, 4912–4918; (d) A. R. Al-Ohaly and J. F. Nixon, *J. Organomet. Chem.*, 1980, **202**, 297–308.

57 Y. S. Duh, C. S. Kao and W. L. Lee, *J. Therm. Anal. Calorim.*, 2017, **127**, 1071–1087.

58 Y. Wang and K. Matyjaszewski, *Macromolecules*, 2010, **43**, 4003–4005.

59 A. J. D. Magenau, Y. Kwak, K. Schröder and K. Matyjaszewski, *ACS Macro Lett.*, 2012, **1**, 508–512.

60 (a) A. D. Asandei, I. W. Moran and C. Bruckner, *Polym. Prepr.*, 2003, **44**(2), 827–828; (b) A. D. Asandei, I. W. Moran and C. Bruckner, *Polym. Prepr.*, 2003, **44**(1), 833–834.

61 Z. Xue and R. Poli, *J. Polym. Sci., Part A: Polym. Chem.*, 2013, **51**, 3494–3504.

62 W. T. Eckenhoff, A. B. Biernesser and T. Pintauer, *Inorg. Chim. Acta*, 2012, **382**, 84.

63 M. Teodorescu, S. G. Gaynor and K. Matyjaszewski, *Macromolecules*, 2000, **33**, 2335–2339.

64 K. Meier and G. Rihs, *Angew. Chem., Int. Ed. Engl.*, 1985, **24**, 858–859.

65 (a) U. Russo, G. Valle, G. L. Long and E. O. Schlemper, *Inorg. Chem.*, 1987, **26**, 665–670; (b) K. B. Yatsimirskii, E. V. Rybak-Akimova and G. G. Talanova, *Dokl. Akad. Nauk Ukr. SSR, Ser. B: Geol., Khim. Biol. Nauki*, 1989, **4**, 50–53.

66 J. Peng, M. Ding, Z. Cheng, L. Zhang and X. Zhu, *RSC Adv.*, 2015, **5**, 104733–104739.

67 T. Alman and R. G. Goel, *Can. J. Chem.*, 1982, **60**, 716–722.

68 (*a*) K. Matyjaszewski, D. A. Shipp, J. L. Wang, T. Grimaud and T. E. Patten, *Macromolecules*, 1998, **31**, 6836–6840; (*b*) C. H. Peng, J. Kong, F. Seeliger and K. Matyjaszewski, *Macromolecules*, 2011, **44**, 7546–7557.

69 M. Wada, S. Higashizaki and A. Tsuboi, *J. Chem. Res., Synop.*, 1985, 38–39.

70 E. C. Alyea, G. Ferguson and S. Kannan, *Polyhedron*, 2000, **19**, 2211–2213.

71 M. Buback and J. Morick, *Macromol. Chem. Phys.*, 2010, **211**, 2154–2161.

72 Y. Wang, H. Schroeder, J. Morick, M. Buback and K. Matyjaszewski, *Macromol. Rapid Commun.*, 2013, **34**, 604–609.